

Adaptive Recursive Decentralized Cooperative Localization for Multirobot Systems With Time-Varying Measurement Accuracy

Yulong Huang¹, Member, IEEE, Chao Xue¹, Fengchi Zhu¹, Wenwu Wang², Senior Member, IEEE, Yonggang Zhang¹, Senior Member, IEEE, and Jonathon A. Chambers³, Fellow, IEEE

Abstract—Decentralized cooperative localization (DCL) is a promising method to determine accurate multirobot poses (i.e., positions and orientations) for robot teams operating in an environment without absolute navigation information. Existing DCL methods often use fixed measurement noise covariance matrices for multirobot pose estimation; however, their performance degrades when the measurement noise covariance matrices are time-varying. To address this problem, in this article, a novel adaptive recursive DCL method is proposed for multi-robot systems with time-varying measurement accuracy. Each robot estimates its pose and measurement noise covariance matrices simultaneously in a decentralized manner based on the constructed hierarchical Gaussian models using the variational Bayesian approach. Simulation and experimental results show that the proposed method has improved cooperative localization accuracy and estimation consistency but slightly heavier computational load than the existing recursive DCL method.

Index Terms—Adaptive filter, decentralized cooperative localization, extended Kalman filter, multirobot systems, variational Bayesian.

I. INTRODUCTION

A. Background

MULTIROBOT systems have been widely used in many applications, such as area exploration [1], [2], region surveillance [3], and fast search and rescue [4]. Accurate positions and orientations (poses) of all the robots are essential for the success of their operation in performing various tasks

Manuscript received October 11, 2020; revised January 2, 2021; accepted January 4, 2021. Date of publication January 25, 2021; date of current version February 11, 2021. This work was supported in part by the National Natural Science Foundation of China under Grant 61903097 and Grant 61773133 and in part by the Fundamental Research Funds for the Central Universities under Grant 3072020CF0404 and Grant 3072020GIP0409. The Associate Editor coordinating the review process was Alessio De Angelis. (Corresponding authors: Yulong Huang; Yonggang Zhang.)

Yulong Huang, Chao Xue, Fengchi Zhu, and Yonggang Zhang are with the College of Intelligent Systems Science and Engineering, Harbin Engineering University, Harbin 150001, China, and also with the Engineering Research Center of Navigation Instruments, Ministry of Education, Harbin 150001, China (e-mail: heuedu@163.com; xc_adjuster@163.com; zfciggins@163.com; zhangyg@hrbeu.edu.cn).

Wenwu Wang is with the Department of Electrical and Electronic Engineering, University of Surrey, Guildford GU2 7XH, U.K. (e-mail: w.wang@surrey.ac.uk).

Jonathon A. Chambers is with the College of Intelligent Systems Science and Engineering, Harbin Engineering University, Harbin 150001, China, and also with the School of Engineering, University of Leicester, Leicester LE1 7RH, U.K. (e-mail: jonathon.chambers@le.ac.uk).

Digital Object Identifier 10.1109/TIM.2021.3054005

[5], [6]. For an environment with accurate and persistent absolute¹ measurements, it is easy to achieve highly accurate estimates of robots' poses. For example, if the global position system (GPS) signal is accessible, the resultant integration of odometry and GPS can provide accurate estimates of robots' poses. However, for an environment with intermittent absolute measurements or without absolute measurements, it is a challenge to achieve accurate estimates of poses [7]. Cooperative localization (CL) is a promising technique to improve the localization accuracy of multirobot systems for the above scenarios [8], [9]. In the CL, each robot is equipped with the proprioceptive and exteroceptive sensors, and the proprioceptive sensors are used to measure the self-motion of each robot, and the exteroceptive sensors are employed to provide the occasionally accessible absolute measurements and the relative measurements between any two mobile robots. In addition, each robot can share its pose information with other robots through a wireless communication module. With CL, the accurate absolute localization information obtained by some team members can be spread to other members through information exchanges and relative measurements, based on which the multirobot systems can achieve improved localization accuracy [8], [10].

B. Related Works

The Bayesian filtering technique plays an important role to fuse the self-motion measurements, the occasionally accessible absolute measurements, and the relative measurements in the CL. A large number of Bayesian filters have been specifically designed for the CL, such as the extended Kalman filter (EKF) [8], the particle filter [11], [12], the maximum likelihood estimation algorithm [13], and the maximum *a posteriori* estimation algorithm [14]. Among these filtering methods, the EKF has been a popular choice due to its satisfactory estimation accuracy, ease of implementation, and relatively low computational complexity [15]. Under the assumption that the motion modeling noise and the absolute and relative measurement noises all have Gaussian distributions, the EKF can achieve almost optimal pose estimates of all team members for overall multirobot systems (except for the first-order linearization errors) [16]. So far, there are two kinds of EKF-based

¹The word "absolute" means that the measurements are taken relative to accurately known reference positions.

CL (CL-EKF) schemes: the EKF-based centralized CL (CCL-EKF) [8], [10], [17]–[21] and the EKF-based decentralized CL (DCL-EKF) [7], [22]–[25].

In the CCL-EKF method, the self-motion measurements (e.g., linear and rotational velocities) and the occasionally accessible absolute and relative measurements (e.g., relative position, bearing, and range) are all sent to a fusion center, based on which the poses of all robots are jointly estimated using the EKF. Although this CL method is able to achieve almost optimal and completely consistent² pose estimates of all robots under assumptions of Gaussian motion and measurement noises, it requires centralized implementations of the EKF and global communications between the fusion center and all robots in the motion and measurement updates. As a result, the CCL-EKF method is prone to failure caused by the local communication faults and suffers from substantial computational complexities, which may limit its practical applications. To improve the CCL-EKF method, some distributed centralized-equivalent CL (DCECL) methods have been proposed [8], [10], [17]–[21]. Roumeliotis and Bekey [8] first proposed a DCECL method, in which the cross correlation of any two robots is decomposed into two half cross correlations, and the two robots maintain and update the two half cross correlations, respectively, and each robot implements the motion update in a distributed manner. This DCECL method can save communications and computations if the motion update frequency is greater than the measurement update frequency. However, it still requires global communications among all robots. To further alleviate the communication requirements, Kia *et al.* [10], [21] proposed an improved DCECL method, where new intermediate local variables are introduced to achieve decentralized implementations of the EKF. Although this method only requires local communications with the adjacent team members, it imposes an additional constraint that the multirobot systems need to have a communication graph with a spanning tree rooted at the interim master in every time step, which limits the scope of CL for multirobot systems.

As a popular alternative to the CL-EKF, the DCL-EKF method can solve the above problems inherent in the CCL-EKF methods, in which each robot serves as a local fusion center and the CL is implemented in a decentralized manner. However, the DCL-EKF method suffers from an important problem of double-counting which treats correlated pose estimates as uncorrelated and uses shared measurements repeatedly so that inconsistent pose estimates of all robots are thereby induced [26]. Covariance intersection (CI) is a standard technique to address this problem [27]–[29]. In the CI technique, the effects of unknown cross correlations are alleviated by inflating the measurement noise variances of all sensors to obtain more consistent state estimates [27], [28]. Many DCL-EKF methods that exploit the CI-technique

(DCL-EKF-CI) have been proposed [7], [22], [23]. Although these DCL-EKF-CI methods can guarantee estimation consistency, their estimated error covariance matrices of pose estimates are overly inflated (i.e., overly conservative) due to the inflations of measurement noise variances, which results in poor CL accuracy. Another strategy for addressing the problem of double counting is to estimate cross correlations. Zhu and Kia [24] proposed an improved DCL-EKF-CI method by estimating and compensating for the unknown cross correlations. However, this method suffers from heavy computational burdens incurred by a constrained numerical optimization problem. On the other hand, Luft *et al.* [25] proposed a recursive DCL-EKF (RDCL-EKF) method, in which every cross correlation is factored as two half cross correlations,³ and each robot estimates its pose and half cross correlations with the other robots recursively. As compared with the improved DCL-EKF-CI method [24], the RDCL-EKF method has better CL accuracy and smaller computational costs. Although the RDCL-EKF method cannot guarantee that the pose estimates are strictly consistent, it exhibits satisfactory estimation consistency [25]. Unfortunately, its estimation accuracy and consistency degrade substantially when inaccurate measurement noise covariance matrices are exploited, as will be detailed in the next section.

C. Motivations for Paper

The absolute and relative measurement noise covariance matrices are important parameters for implementing the RDCL-EKF method, which will be shown in our simulation and experimental study. In practical multirobot CL applications, the absolute and relative measurement noise covariance matrices are commonly selected as fixed nominal values according to engineering experience. However, the measurement noise covariance matrices may be time-varying, which cannot be matched by fixed nominal values. For example, the measurement accuracy of a camera depends heavily on the distance between the camera and the measured target, and the greater the distance, the worse the measurement accuracy that is achieved and vice versa. As a result, the RDCL-EKF will exhibit poor CL accuracy and estimation consistency when inaccurate nominal absolute and relative measurement noise covariance matrices are used. Although some adaptive Kalman filters [30]–[39] have been proposed to estimate inaccurate noise covariance matrices, these methods are not suitable for the DCL of multi-robot systems since they are specially designed for a single linear system. To the best of the authors' knowledge, the adaptive DCL methods for multirobot systems have not been previously reported.

D. Contributions and Organizations of Paper

To improve the performance of the existing RDCL-EKF method for multirobot systems with time-varying measurement accuracy, a novel adaptive RDCL-EKF method is proposed in this article, in which each robot estimates its pose and

²Suppose that $\hat{\mathbf{x}}$ and \mathbf{P} are, respectively, the estimate and estimated error covariance matrix of a random state vector \mathbf{x} . The state estimate pair $(\hat{\mathbf{x}}, \mathbf{P})$ is consistent if the difference between the estimated error covariance matrix and the real error covariance matrix is positive semidefinite, i.e., $\mathbf{P} - \mathbf{E}[(\mathbf{x} - \hat{\mathbf{x}})(\mathbf{x} - \hat{\mathbf{x}})^T] \geq \mathbf{0}$, and completely consistent if the estimated error covariance matrix is identical to the real error covariance matrix, i.e., $\mathbf{P} = \mathbf{E}[(\mathbf{x} - \hat{\mathbf{x}})(\mathbf{x} - \hat{\mathbf{x}})^T]$.

³Suppose that Σ^{xy} is the cross correlation of random variables \mathbf{x} and \mathbf{y} . If the cross correlation Σ^{xy} can be factored as $\Sigma^{xy} = \Sigma^{xy}(\Sigma^{yx})^T$, then both Σ^{xy} and Σ^{yx} are termed half cross correlations of random variables \mathbf{x} and \mathbf{y} .

absolute and relative measurement noise covariance matrices simultaneously in a decentralized manner. The measurement noise covariance matrices are modeled as inverse-Wishart distributed, from which hierarchical Gaussian models for multirobot systems can be constructed. For each robot, the posterior probability density functions (PDFs) of its pose and measurement noise covariance matrices are mutually coupled under the constructed hierarchical Gaussian models, and the variational Bayesian (VB) approach is therefore employed to obtain approximate joint estimates. The proposed adaptive RDCL-EKF method has the same communication mode as the standard RDCL-EKF method, but only requires slightly higher communication overhead to transmit additional parameters in each cooperation. A large number of simulation and experimental results demonstrate that the proposed adaptive RDCL-EKF method has better CL accuracy and estimation consistency but slightly heavier computational load than the existing RDCL-EKF method for multirobot systems with time-varying measurement accuracy.

This article is organized as follows. In Section II, the multirobot CL model and problem statement are presented. In Section III, the proposed adaptive RDCL-EKF method is derived, and its detailed implementations are given. The simulation and experiment studies are, respectively, provided in Sections IV and V. Conclusions are drawn in Section VI.

II. PRELIMINARIES AND PROBLEM STATEMENT

A. Multirobot CL Models

Consider a cluster of n_R homogeneous or heterogeneous mobile robots moving in a two-dimensional environment with n_L known landmarks. Every mobile robot installs proprioceptive sensors (e.g., wheel-encoders) and exteroceptive sensors (e.g., ultrawide bands (UWB), cameras or laser scanners), in which the proprioceptive sensors are used to measure self-motion of every mobile robot, and the exteroceptive sensors are employed to collect the absolute measurements from the robot to the landmarks or relative measurements from the robot to other robots. The nonlinear discrete-time motion model of robot i can be formulated as follows [7]:

$$\begin{cases} x_k^i = x_{k-1}^i + \left(V_k^i - w_k^{V_i} \right) \cos(\phi_{k-1}^i) \Delta t \\ y_k^i = y_{k-1}^i + \left(V_k^i - w_k^{V_i} \right) \sin(\phi_{k-1}^i) \Delta t \\ \phi_k^i = \phi_{k-1}^i + \left(\Omega_k^i - w_k^{\Omega_i} \right) \Delta t \end{cases} \quad (1)$$

where x_k^i , y_k^i and ϕ_k^i are, respectively, the east and north positions and orientation of robot i at time k , and $[x_k^i, y_k^i, \phi_k^i]$ denotes the pose of robot i at time k , and V_k^i and Ω_k^i are the measured linear and rotational velocities of robot i at time k provided by the proprioceptive sensors with measurement noises $w_k^{V_i}$ and $w_k^{\Omega_i}$, respectively, and Δt denotes the discretization time.

In this article, three kinds of absolute and relative measurements are considered, including the relative position, bearing, and range measurements. For robot i , its three kinds of measurement models from robot i to landmark l are written

as [7], [8]

$$\begin{cases} \mathbf{p}_{ak}^{il} = \mathbf{C}^T(\phi_k^i) \begin{bmatrix} x_L^l - x_k^i \\ y_L^l - y_k^i \end{bmatrix} + \mathbf{v}_{pak}^{il} \\ \theta_{ak}^{il} = \text{atan2}(y_k^i - y_L^l, x_k^i - x_L^l) - \phi_k^i + v_{\theta_{ak}}^{il} \\ r_{ak}^{il} = \sqrt{(x_k^i - x_L^l)^2 + (y_k^i - y_L^l)^2} + v_{r_{ak}}^{il} \end{cases} \quad (2)$$

where the superscript ‘‘T’’ denotes the transpose operation of a matrix, and the subscript ‘‘ak’’ denotes the absolute measurement at time k , and \mathbf{p}_{ak}^{il} , θ_{ak}^{il} and r_{ak}^{il} are the relative position,⁴ bearing, and range measurements from robot i to landmark l at time k measured by the exteroceptive sensors with measurement noises \mathbf{v}_{pak}^{il} , $v_{\theta_{ak}}^{il}$ and $v_{r_{ak}}^{il}$, respectively, and x_L^l and y_L^l denote the east and north positions of landmark l with the subscript ‘‘L’’ denoting the landmark, and $\mathbf{C}(\phi_k^i)$ denotes the direction cosine matrix from the local framework of robot i to the global framework, which is given by

$$\mathbf{C}(\phi_k^i) = \begin{bmatrix} \cos(\phi_k^i) & -\sin(\phi_k^i) \\ \sin(\phi_k^i) & \cos(\phi_k^i) \end{bmatrix}. \quad (3)$$

It is noted that the landmarks are all assumed to be static, and their positions are accurately known in the models (2).

Similarly, for robot i , its three kinds of relative measurement models to robot j are given by [7], [8]

$$\begin{cases} \mathbf{p}_{rk}^{ij} = \mathbf{C}^T(\phi_k^i) \begin{bmatrix} x_k^j - x_k^i \\ y_k^j - y_k^i \end{bmatrix} + \mathbf{v}_{prk}^{ij} \\ \theta_{rk}^{ij} = \text{atan2}(y_k^i - y_k^j, x_k^i - x_k^j) - \phi_k^i + v_{\theta_{rk}}^{ij} \\ r_{rk}^{ij} = \sqrt{(x_k^i - x_k^j)^2 + (y_k^i - y_k^j)^2} + v_{r_{rk}}^{ij} \end{cases} \quad (4)$$

where the subscript ‘‘rk’’ denotes the relative measurement at time k , and the superscript ‘‘ij’’ means that robot i is relative to robot j , and \mathbf{p}_{rk}^{ij} , θ_{rk}^{ij} and r_{rk}^{ij} are the relative position, bearing, and range measurements of robot i to robot j at time k measured by the exteroceptive sensors with measurement noises \mathbf{v}_{prk}^{ij} , $v_{\theta_{rk}}^{ij}$ and $v_{r_{rk}}^{ij}$, respectively, and x_k^j and y_k^j are, respectively, the east and north positions of robot j at time k .

Define the pose of robot i as its state vector, i.e., $\mathbf{x}_k^i \triangleq [x_k^i, y_k^i, \phi_k^i]^T$. The motion model and absolute and relative measurement models of robot i can be, respectively, formulated as the following general forms:

$$\begin{cases} \mathbf{x}_k^i = \mathbf{f}_k^i(\mathbf{x}_{k-1}^i, \mathbf{w}_k^i) \\ \mathbf{z}_{ak}^{il} = \mathbf{h}_{ak}^{il}(\mathbf{x}_k^i, \mathbf{x}_L^l) + \mathbf{v}_{ak}^{il} \\ \mathbf{z}_{rk}^{ij} = \mathbf{h}_{rk}^{ij}(\mathbf{x}_k^i, \mathbf{x}_k^j) + \mathbf{v}_{rk}^{ij} \end{cases} \quad (5)$$

where $\mathbf{z}_{ak}^{il} \in \mathbf{R}^{n_a}$ and $\mathbf{z}_{rk}^{ij} \in \mathbf{R}^{n_r}$ are, respectively, the absolute and relative measurement vectors to landmark l and robot j , and $\mathbf{x}_L^l \triangleq [x_L^l, y_L^l]^T$ is the position of landmark l , and $\mathbf{f}_k^i(\cdot)$, $\mathbf{h}_{ak}^{il}(\cdot)$ and $\mathbf{h}_{rk}^{ij}(\cdot)$ are, respectively, the state evolution function and the absolute and relative measurement functions, which are correspondingly defined according to (1), (2), and (4), and $\mathbf{w}_k^i \triangleq [w_k^{V_i}, w_k^{\Omega_i}]^T$, \mathbf{v}_{ak}^{il} and \mathbf{v}_{rk}^{ij} are, respectively, the state noise and the absolute and relative measurement noises. In this article, \mathbf{w}_k^i , \mathbf{v}_{ak}^{il} and \mathbf{v}_{rk}^{ij} are all assumed to be zero-mean

⁴Here, the relative position \mathbf{p}_{ak}^{il} is an absolute measurement since it is taken from robot i to landmark l whose position is accurately known.

TABLE I
LOCAL MOTION UPDATE FOR ROBOT i [25]

Function 1: $\left(\hat{\mathbf{x}}_{k|k-1}^i, \Sigma_{k|k-1}^i, \left\{ \sigma_{k|k-1}^{ij} \right\}_{\substack{\{j \neq i\} \\ \{1 \leq j \leq n_R\}}} \right) = \text{LMU} \left(\hat{\mathbf{x}}_{k-1|k-1}^i, \Sigma_{k-1|k-1}^i, \left\{ \sigma_{k-1|k-1}^{ij} \right\}_{\substack{\{j \neq i\} \\ \{1 \leq j \leq n_R\}}}, \mathbf{Q}_k^i \right)$

Calculate:

1. Predicted state vector (pose): $\hat{\mathbf{x}}_{k|k-1}^i = \mathbf{f}_k^i(\hat{\mathbf{x}}_{k-1|k-1}^i, \mathbf{0})$
2. State Jacobi matrix: $\mathbf{F}_k^i = \frac{\partial \mathbf{f}_k^i(\mathbf{x}_{k-1}^i, \mathbf{w}_k^i)}{\partial \mathbf{x}_{k-1}^i}(\hat{\mathbf{x}}_{k-1|k-1}^i, \mathbf{0})$
3. State noise Jacobi matrix: $\mathbf{G}_k^i = \frac{\partial \mathbf{f}_k^i(\mathbf{x}_{k-1}^i, \mathbf{w}_k^i)}{\partial \mathbf{w}_k^i}(\hat{\mathbf{x}}_{k-1|k-1}^i, \mathbf{0})$
4. Prediction error covariance matrix: $\Sigma_{k|k-1}^i = \mathbf{F}_k^i \Sigma_{k-1|k-1}^i (\mathbf{F}_k^i)^T + \mathbf{G}_k^i \mathbf{Q}_k^i (\mathbf{G}_k^i)^T$
5. Predicted half cross-correlations:

for $j = 1 : n_R, j \neq i$ **do**

$$\sigma_{k|k-1}^{ij} = \mathbf{F}_k^i \sigma_{k-1|k-1}^{ij}$$

end for

Gaussian white distributed, that is $\mathbf{w}_k^i \sim \mathbf{N}(\mathbf{0}, \mathbf{Q}_k^i)$, $\mathbf{v}_{ak}^{il} \sim \mathbf{N}(\mathbf{0}, \mathbf{R}_{ak}^{il})$, and $\mathbf{v}_{rk}^{ij} \sim \mathbf{N}(\mathbf{0}, \mathbf{R}_{rk}^{ij})$, where \mathbf{Q}_k^i , \mathbf{R}_{ak}^{il} , and \mathbf{R}_{rk}^{ij} are, respectively, the state noise covariance matrix and the absolute and relative measurement noise covariance matrices. Furthermore, \mathbf{w}_k^i , \mathbf{v}_{ak}^{il} and \mathbf{v}_{rk}^{ij} are all assumed to be uncorrelated with each other.

B. Problem Statement

Before presenting the main motivation of this article, the existing RDCL-EKF algorithm [25] is first reviewed. In the RDCL-EKF method, the heart is to estimate beliefs $\{\hat{\mathbf{x}}_{k|k}^i, \Sigma_{k|k}^i\}_{\{1 \leq i \leq n_R\}}$ and cross correlations $\{\Sigma_{k|k}^{ij}\}_{\substack{\{j \neq i\} \\ \{1 \leq j \leq n_R\}}}$ of all robots based on a decentralized strategy, where the cross correlation $\Sigma_{k|k}^{ij}$ is factored as two half cross correlations, that is $\Sigma_{k|k}^{ij} = \Sigma_{k|k}^{ij} (\Sigma_{k|k}^{ji})^T$, and the half cross correlations $\Sigma_{k|k}^{ij}$ and $\Sigma_{k|k}^{ji}$ are recursively estimated and maintained by robots i and j , respectively. For robot i , it requires to estimate its own belief $\{\hat{\mathbf{x}}_{k|k}^i, \Sigma_{k|k}^i\}$ and half cross correlations $\{\Sigma_{k|k}^{ij}\}_{\substack{\{j \neq i\} \\ \{1 \leq j \leq n_R\}}}$ with the remaining $(n_R - 1)$ robots. The RDCL-EKF algorithm consists of three parts: the local motion update (LMU), the local absolute measurement update (LAMU), and the cooperative relative measurement update (CRMU), which are, respectively, summarized as three functions in Tables I–III. In Tables II and III, l_k^{i*} and j_k^{i*} , respectively, denote the landmark set and the robot set detected by robot i at time k , and $\text{row}\{\mathbf{a}_l\}_{l \in \Gamma}$, $\text{col}\{\mathbf{a}_l\}_{l \in \Gamma}$, and $\text{diag}\{\mathbf{a}_l\}_{l \in \Gamma}$ denote the block row matrix, the block column matrix, and the block diagonal matrix, respectively, which are composed of all matrices in the set $\{\mathbf{a}_l | l \in \Gamma\}$.

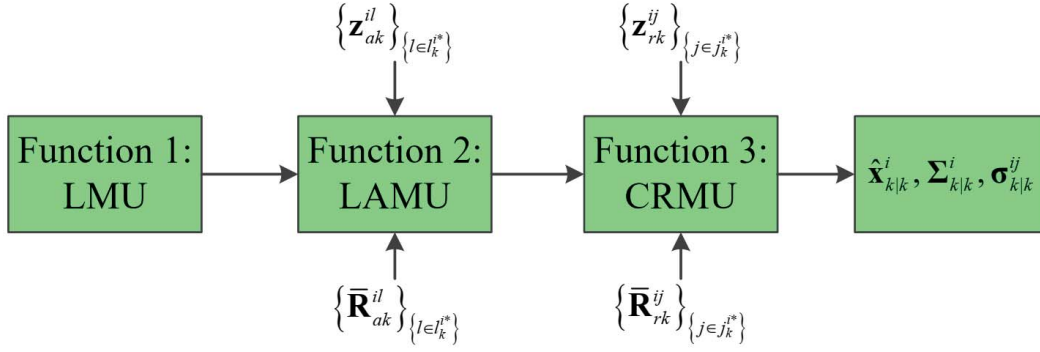
It is seen from Tables II and III that the absolute and relative measurement noise covariance matrices $\{\mathbf{R}_{ak}^{il}\}_{\{l \in l_k^{i*}\}}$ and $\{\mathbf{R}_{rk}^{ij}\}_{\{j \in j_k^{i*}\}}$ are, respectively, the inputs of the LAMU

and the CRMU functions. Both the state estimate $\hat{\mathbf{x}}_{k|k}^i$ and estimation error covariance matrix $\Sigma_{k|k}^i$ depend on $\{\mathbf{R}_{ak}^{il}\}_{\{l \in l_k^{i*}\}}$ and $\{\mathbf{R}_{rk}^{ij}\}_{\{j \in j_k^{i*}\}}$, and then the state estimation accuracy relies on the accuracies of $\{\mathbf{R}_{ak}^{il}\}_{\{l \in l_k^{i*}\}}$ and $\{\mathbf{R}_{rk}^{ij}\}_{\{j \in j_k^{i*}\}}$. Meanwhile, the half cross correlations $\{\Sigma_{k|k}^{ij}\}_{\substack{\{j \neq i\} \\ \{1 \leq j \leq n_R\}}}$ depend on $\{\mathbf{R}_{ak}^{il}\}_{\{l \in l_k^{i*}\}}$ and $\{\mathbf{R}_{rk}^{ij}\}_{\{j \in j_k^{i*}\}}$, which means that the accuracies of $\{\mathbf{R}_{ak}^{il}\}_{\{l \in l_k^{i*}\}}$ and $\{\mathbf{R}_{rk}^{ij}\}_{\{j \in j_k^{i*}\}}$ also have effects on the estimation consistency. In practical multirobot CL applications, the measurement accuracy of exteroceptive sensors may be time-varying. For example, the measurement accuracy of a camera depends heavily on the distance between the camera and the measured target, and the greater the distance, the worse the measurement accuracy that is achieved and vice versa. However, the absolute and relative measurement noise covariance matrices $\{\mathbf{R}_{ak}^{il}\}_{\{l \in l_k^{i*}\}}$ and $\{\mathbf{R}_{rk}^{ij}\}_{\{j \in j_k^{i*}\}}$ are commonly selected as fixed nominal values $\{\bar{\mathbf{R}}_{ak}^{il}\}_{\{l \in l_k^{i*}\}}$ and $\{\bar{\mathbf{R}}_{rk}^{ij}\}_{\{j \in j_k^{i*}\}}$ according to engineering experience, as shown in Fig. 1. As a result, poor CL accuracy and serious estimation inconsistency will be induced by the use of inaccurate nominal values $\{\bar{\mathbf{R}}_{ak}^{il}\}_{\{l \in l_k^{i*}\}}$ and $\{\bar{\mathbf{R}}_{rk}^{ij}\}_{\{j \in j_k^{i*}\}}$ in the LAMU and CRMU functions, which represents the main motivation of this article.

III. NOVEL ADAPTIVE RDCL-EKF METHOD

A. Design Idea of the Proposed Method

In this article, to improve the CL accuracy and estimation consistency, a novel adaptive RDCL-EKF method is proposed, in which the absolute and relative measurement noise covariance matrices are adaptively estimated based on the VB approach. For multirobot systems, any mobile robot i may detect any landmark l , and the absolute measurement noise covariance matrix \mathbf{R}_{ak}^{il} is required in the LAMU if the

Fig. 1. Diagram of existing RDCL-EKF algorithm for robot i .TABLE II
LAMU FOR ROBOT i [25]

$$\text{Function 2: } \left(\hat{\mathbf{x}}_{k|k}^{i(a)}, \Sigma_{k|k}^{i(a)}, \left\{ \sigma_{k|k}^{ij(a)} \right\}_{\substack{j \neq i \\ 1 \leq j \leq n_R}} \right) = \text{LAMU} \left(\hat{\mathbf{x}}_{k|k-1}^i, \Sigma_{k|k-1}^i, \left\{ \sigma_{k|k-1}^{ij} \right\}_{\substack{j \neq i \\ 1 \leq j \leq n_R}}, l_k^{i*}, \left\{ \mathbf{z}_{ak}^{il}, \mathbf{R}_{ak}^{il}, \mathbf{x}_L^l \right\}_{l \in l_k^{i*}} \right)$$

If the detected landmark set l_k^{i*} of robot i is non-empty:

Construct:

1. Augmented absolute measurement: $\mathbf{z}_{ak}^{il_k^{i*}} = \text{col} \left\{ \mathbf{z}_{ak}^{il} \right\}_{l \in l_k^{i*}}$
2. Augmented absolute measurement noise covariance matrix: $\mathbf{R}_{ak}^{il_k^{i*}} = \text{diag} \left\{ \mathbf{R}_{ak}^{il} \right\}_{l \in l_k^{i*}}$

Calculate:

3. Augmented absolute measurement Jacobi matrix: $\mathbf{H}_{ak}^{il_k^{i*}} = \text{row} \left\{ \mathbf{H}_{ak}^{il} \right\}_{l \in l_k^{i*}}$, where $\mathbf{H}_{ak}^{il} = \frac{\partial \mathbf{h}_{ak}^{il}(\mathbf{x}_k^i, \mathbf{x}_L^l)}{\partial \mathbf{x}_k^i} \left(\hat{\mathbf{x}}_{k|k-1}^i \right)$
4. Kalman gain of augmented absolute measurement: $\mathbf{K}_{ak}^{il_k^{i*}} = \Sigma_{k|k-1}^i \left(\mathbf{H}_{ak}^{il_k^{i*}} \right)^T \left[\mathbf{H}_{ak}^{il_k^{i*}} \Sigma_{k|k-1}^i \left(\mathbf{H}_{ak}^{il_k^{i*}} \right)^T + \mathbf{R}_{ak}^{il_k^{i*}} \right]^{-1}$
5. Predicted augmented absolute measurement: $\hat{\mathbf{z}}_{ak|k-1}^{il_k^{i*}} = \text{col} \left\{ \hat{\mathbf{z}}_{ak|k-1}^{il} \right\}_{l \in l_k^{i*}}$, where $\hat{\mathbf{z}}_{ak|k-1}^{il} = \mathbf{h}_{ak}^{il} \left(\hat{\mathbf{x}}_{k|k-1}^i, \mathbf{x}_L^l \right)$
6. State estimate: $\hat{\mathbf{x}}_{k|k}^{i(a)} = \hat{\mathbf{x}}_{k|k-1}^i + \mathbf{K}_{ak}^{il_k^{i*}} \left[\mathbf{z}_{ak}^{il_k^{i*}} - \hat{\mathbf{z}}_{ak|k-1}^{il_k^{i*}} \right]$
7. Estimation error covariance matrix of LAMU: $\Sigma_{k|k}^{i(a)} = \left[\mathbf{I} - \mathbf{K}_{ak}^{il_k^{i*}} \mathbf{H}_{ak}^{il_k^{i*}} \right] \Sigma_{k|k-1}^i$
8. Estimated half cross-correlations:

for $j = 1 : n_R, j \neq i$ **do**

$$\sigma_{k|k}^{ij(a)} = \left[\mathbf{I} - \mathbf{K}_{ak}^{il_k^{i*}} \mathbf{H}_{ak}^{il_k^{i*}} \right] \sigma_{k|k-1}^{ij}$$

end for

If the detected landmark set l_k^{i*} of robot i is empty: $\hat{\mathbf{x}}_{k|k}^{i(a)} = \hat{\mathbf{x}}_{k|k-1}^i, \Sigma_{k|k}^{i(a)} = \Sigma_{k|k-1}^i, \left\{ \sigma_{k|k}^{ij(a)} = \sigma_{k|k-1}^{ij} \right\}_{\substack{j \neq i \\ 1 \leq j \leq n_R}}$

mobile robot i detects the landmark l , where $1 \leq i \leq n_R$ and $1 \leq l \leq n_L$. Since each mobile robot has different running statuses and each landmark has different positions, $n_R \times n_L$ absolute measurement noise covariance matrices must be adaptively estimated for the entire system, which are shown in Fig. 2. It is seen from Fig. 2 that all absolute measurement noise covariance matrices are mutually independent so that they can be separately estimated. On the other hand, any mobile robot i may detect any mobile robot j , and the relative measurement noise covariance matrix \mathbf{R}_{rk}^{ij} is required in the CRMU if the mobile robot i detects the mobile robot j , where

$1 \leq i, j \leq n_R$ and $i \neq j$. Considering that \mathbf{R}_{rk}^{ij} and \mathbf{R}_{rk}^{ji} are identical, then only $n_R(n_R - 1)/2$ relative measurement noise covariance matrices are unknown for the entire system, which are illustrated in Fig. 3. An intuitive method is that the robots i and j estimate the relative measurement noise covariance matrix \mathbf{R}_{rk}^{ij} ($i < j$) together based on the measurements \mathbf{z}_{rk}^{ij} and \mathbf{z}_{rk}^{ji} . However, a fusion center is required to collect the relative measurements \mathbf{z}_{rk}^{ij} and \mathbf{z}_{rk}^{ji} for estimating \mathbf{R}_{rk}^{ij} , which violates the original intention of recursive DCL (RDCL).

To address the above problem, in this article, a decentralized estimation strategy is proposed to estimate the relative

TABLE III
CRMU FOR ROBOT i [25]

Function 3: $\left(\hat{\mathbf{x}}_{k|k}^i, \Sigma_{k|k}^i, \left\{ \sigma_{k|k}^{ij} \right\}_{\substack{j \neq i \\ 1 \leq j \leq n_R}} \right) = \text{CRMU} \left(\hat{\mathbf{x}}_{k|k}^{i(a)}, \Sigma_{k|k}^{i(a)}, \left\{ \sigma_{k|k}^{ij(a)} \right\}_{\substack{j \neq i \\ 1 \leq j \leq n_R}}, J_k^{i*}, \left\{ \mathbf{z}_{rk}^{ij}, \mathbf{R}_{rk}^{ij} \right\}_{j \in J_k^{i*}} \right)$

If the detected robot set J_k^{i*} of robot i is non-empty:

1. Receive information from robots in J_k^{i*} : $\left\{ \hat{\mathbf{x}}_{k|k}^{j(a)}, \Sigma_{k|k}^{j(a)}, \sigma_{k|k}^{js(a)} \right\}_{\substack{s \neq j \in J_k^{i*} \\ 1 \leq s \leq n_R}}$

Construct:

2. Augmented state estimate of robots in J_k^{i*} : $\hat{\mathbf{x}}_{k|k}^{j_k^{i*}(a)} = \text{col} \left\{ \hat{\mathbf{x}}_{k|k}^{j(a)} \right\}_{j \in J_k^{i*}}$
3. Augmented estimation error covariance matrix of robots in J_k^{i*} : $\Sigma_{k|k}^{j_k^{i*}(a)} = \text{block} \left\{ \Sigma_{k|k}^{j(a)}, \Sigma_{k|k}^{js(a)} \right\}_{\substack{s \neq j \\ \{s, j \in J_k^{i*}\}}}$,

where $\Sigma_{k|k}^{js(a)} = \sigma_{k|k}^{js(a)} \left(\sigma_{k|k}^{js(a)} \right)^T$.

4. Augmented relative measurement: $\mathbf{z}_{rk}^{ij_k^{i*}} = \text{col} \left\{ \mathbf{z}_{rk}^{ij} \right\}_{j \in J_k^{i*}}$
5. Augmented relative measurement noise covariance matrix: $\mathbf{R}_{rk}^{ij_k^{i*}} = \text{diag} \left\{ \mathbf{R}_{rk}^{ij} \right\}_{j \in J_k^{i*}}$

Calculate:

6. Cross-correlation of robot i and robots in J_k^{i*} : $\Sigma_{k|k}^{ij_k^{i*}(a)} = \text{row} \left\{ \Sigma_{k|k}^{ij(a)} \right\}_{j \in J_k^{i*}}$, where $\Sigma_{k|k}^{ij(a)} = \sigma_{k|k}^{ij(a)} \left(\sigma_{k|k}^{ji(a)} \right)^T$
7. Augmented estimation error covariance matrix of robot i and robots in J_k^{i*} : $\Sigma_{k|k}^{(a)} = \begin{bmatrix} \Sigma_{k|k}^i & \Sigma_{k|k}^{ij_k^{i*}(a)} \\ \left(\Sigma_{k|k}^{ij_k^{i*}(a)} \right)^T & \Sigma_{k|k}^{j_k^{i*}(a)} \end{bmatrix}$
8. Augmented measurement Jacobi matrix of robot i and robots in J_k^{i*} : $\mathbf{H}_{rk}^{ij_k^{i*}} = \text{row} \left\{ \mathbf{H}_{rk}^i, \mathbf{H}_{rk}^j \right\}_{j \in J_k^{i*}}$,
where $\mathbf{H}_{rk}^i = \frac{\partial \mathbf{h}_{rk}^{ij}(\mathbf{x}_k^i, \mathbf{x}_k^j)}{\partial \mathbf{x}_k^i} \left(\hat{\mathbf{x}}_{k|k}^{i(a)}, \hat{\mathbf{x}}_{k|k}^{j(a)} \right)$ and $\mathbf{H}_{rk}^j = \frac{\partial \mathbf{h}_{rk}^{ij}(\mathbf{x}_k^i, \mathbf{x}_k^j)}{\partial \mathbf{x}_k^j} \left(\hat{\mathbf{x}}_{k|k}^{i(a)}, \hat{\mathbf{x}}_{k|k}^{j(a)} \right)$
9. Kalman gain of augmented relative measurement: $\mathbf{K}_{rk}^{ij_k^{i*}} = \Sigma_{k|k}^{(a)} \left(\mathbf{H}_{rk}^{ij_k^{i*}} \right)^T \left[\mathbf{H}_{rk}^{ij_k^{i*}} \Sigma_{k|k}^{(a)} \left(\mathbf{H}_{rk}^{ij_k^{i*}} \right)^T + \mathbf{R}_{rk}^{ij_k^{i*}} \right]^{-1}$
10. Predicted augmented relative measurement: $\hat{\mathbf{z}}_{rk|k-1}^{ij_k^{i*}} = \text{col} \left\{ \hat{\mathbf{z}}_{rk|k-1}^{ij} \right\}_{j \in J_k^{i*}}$, where $\hat{\mathbf{z}}_{rk|k-1}^{ij} = \mathbf{h}_{rk}^{ij} \left(\hat{\mathbf{x}}_{k|k-1}^{i(a)}, \hat{\mathbf{x}}_{k|k-1}^{j(a)} \right)$
11. State estimate: $\begin{bmatrix} \hat{\mathbf{x}}_{k|k}^i \\ \hat{\mathbf{x}}_{k|k}^{j_k^{i*}} \end{bmatrix} = \begin{bmatrix} \hat{\mathbf{x}}_{k|k}^{i(a)} \\ \hat{\mathbf{x}}_{k|k}^{j_k^{i*}(a)} \end{bmatrix} + \mathbf{K}_{rk}^{ij_k^{i*}} \left[\mathbf{z}_{rk}^{ij_k^{i*}} - \hat{\mathbf{z}}_{rk|k-1}^{ij_k^{i*}} \right]$
12. Estimation error covariance matrix: $\begin{bmatrix} \Sigma_{k|k}^i & \Sigma_{k|k}^{ij_k^{i*}} \\ \left(\Sigma_{k|k}^{ij_k^{i*}} \right)^T & \Sigma_{k|k}^{j_k^{i*}} \end{bmatrix} = \left(\mathbf{I} - \mathbf{K}_{rk}^{ij_k^{i*}} \mathbf{H}_{rk}^{ij_k^{i*}} \right) \Sigma_{k|k}^{(a)}$
13. Estimated half cross-correlations of robot i : $\left\{ \sigma_{k|k}^{ij} = \Sigma_{k|k}^{ij} \right\}_{j \in J_k^{i*}}$

for $t = 1 : n_R, t \notin \{i, j_k^{i*}\}$ do

$$\sigma_{k|k}^{it} = \Sigma_{k|k}^i \left(\Sigma_{k|k}^{i(a)} \right)^{-1} \sigma_{k|k}^{it(a)}$$

end for

If robot i is detected by robot j : Send information to robot j : $\hat{\mathbf{x}}_{k|k}^{i(a)}, \Sigma_{k|k}^{i(a)}, \sigma_{k|k}^{ij(a)}$; Receive information from robot j : $\hat{\mathbf{x}}_{k|k}^j, \Sigma_{k|k}^j, \sigma_{k|k}^{jj} = \mathbf{I}$; Calculate the estimated half cross-correlations of robot i :

for $t = 1 : n_R, t \notin \{i, j\}$ do

$$\sigma_{k|k}^{it} = \Sigma_{k|k}^i \left(\Sigma_{k|k}^{i(a)} \right)^{-1} \sigma_{k|k}^{it(a)}$$

end for

If robot i doesn't cooperate with any robots: $\hat{\mathbf{x}}_{k|k}^i = \hat{\mathbf{x}}_{k|k}^{i(a)}, \Sigma_{k|k}^i = \Sigma_{k|k}^{i(a)}, \left\{ \sigma_{k|k}^{ij} = \sigma_{k|k}^{ij(a)} \right\}_{\substack{j \neq i \\ 1 \leq j \leq n_R}}$

measurement noise covariance matrices, in which each pair of relative measurement noise covariance matrices $\{\mathbf{R}_{rk}^{ij}, \mathbf{R}_{rk}^{ji}\}$ ($i < j$) is sequentially estimated and updated. That is to say, if robot j is first detected by robot i , then \mathbf{R}_{rk}^{ij} is estimated

based on the relative measurement \mathbf{z}_{rk}^{ij} and the estimation information of \mathbf{R}_{rk}^{ij} is sent from robot i to robot j . Next, if robot i is detected by robot j , then \mathbf{R}_{rk}^{ji} is estimated based on the relative measurement \mathbf{z}_{rk}^{ji} and the received estimation

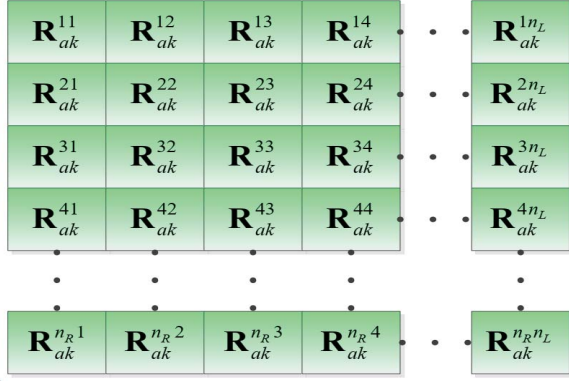


Fig. 2. All absolute measurement noise covariance matrices for the entire system.

information of \mathbf{R}_{rk}^{ij} . Finally, the estimation information of \mathbf{R}_{rk}^{ji} is sent from robot j to robot i to replace the previous estimation information of \mathbf{R}_{rk}^{ij} , and the estimate of \mathbf{R}_{rk}^{ij} is further refined. The diagram of the proposed decentralized estimation strategy for $\{\mathbf{R}_{rk}^{ij}, \mathbf{R}_{rk}^{ji}\}$ is shown in Fig. 4. It can be seen from Fig. 4 that the proposed decentralized estimation strategy can guarantee that the constraint $\mathbf{R}_{rk}^{ij} = \mathbf{R}_{rk}^{ji}$ holds, and both the relative measurements \mathbf{z}_{rk}^{ij} and \mathbf{z}_{rk}^{ji} are used to estimate the relative measurement noise covariance matrices $\{\mathbf{R}_{rk}^{ij}, \mathbf{R}_{rk}^{ji}\}$.

The diagram of the proposed RDCL-EKF method for robot i is illustrated in Fig. 5, where $\{\hat{\mathbf{R}}_{ak}^{il}\}_{l \in l_k^{i*}}$ and $\{\hat{\mathbf{R}}_{rk}^{ij}\}_{j \in j_k^{i*}}$ denote the estimated values of the absolute and relative measurement noise covariance matrices, respectively. We can observe from Fig. 5 that, for the proposed method, the absolute and relative measurement noise covariance matrices are adaptively estimated in a sequential manner. First, the state vector (pose) \mathbf{x}_k^i of robot i and the absolute measurement noise covariance matrix $\{\mathbf{R}_{ak}^{il}\}_{l \in l_k^{i*}}$ are jointly estimated based on the previous measurements $\mathbf{z}_{1:k-1}$ and the current absolute measurement $\{\mathbf{z}_{ak}^{il}\}_{l \in l_k^{i*}}$ using the VB approach in the LAMU, where $\mathbf{z}_{1:k-1}$ denotes the set of all available absolute and relative measurements from time 1 to time $k-1$. Then, the state vector (pose) \mathbf{x}_k^i of robot i and the relative measurement noise covariance matrix $\{\mathbf{R}_{rk}^{ij}\}_{j \in j_k^{i*}}$ are jointly estimated based on the previous measurements $\mathbf{z}_{1:k-1}$, the current absolute measurement $\{\mathbf{z}_{ak}^{il}\}_{l \in l_k^{i*}}$, and the current relative measurement $\{\mathbf{z}_{rk}^{ij}\}_{j \in j_k^{i*}}$ using the VB approach in the CRMU. As compared with the existing RDCL-EKF method, the proposed method can achieve better CL accuracy and estimation consistency via adaptively estimating the absolute and relative measurement noise covariance matrices. Next, we will present the statistical modeling of the state vector and the measurement noise covariance matrices.

B. Statistical Modeling

In the RDCL-EKF framework, the one-step prediction PDF of robot i is approximated as Gaussian, that is

$$p(\mathbf{x}_k^i | \mathbf{z}_{1:k-1}) = N(\mathbf{x}_k^i; \hat{\mathbf{x}}_{k|k-1}^i, \Sigma_{k|k-1}^i) \quad (6)$$

where $\hat{\mathbf{x}}_{k|k-1}^i$ and $\Sigma_{k|k-1}^i$ can be obtained using the LMU function in Table I.

According to the absolute measurement model in (5), the absolute measurement likelihood PDF of robot i relative to landmark l can be formulated as

$$p(\mathbf{z}_{ak}^{il} | \mathbf{x}_k^i, \mathbf{R}_{ak}^{il}) = N(\mathbf{z}_{ak}^{il}; \mathbf{h}_{ak}^{il}(\mathbf{x}_k^i, \mathbf{x}_L^l), \mathbf{R}_{ak}^{il}), \quad l \in l_k^{i*} \quad (7)$$

where the absolute measurement noise covariance matrix \mathbf{R}_{ak}^{il} is assumed as a random variable. In Bayesian statistics, the inverse-Wishart distribution is often used as a conjugate prior distribution of the covariance matrix of a Gaussian distribution with known mean value, which can guarantee the conjugate inference under the variational inference framework [40]. Motivated by this fact, the absolute measurement noise covariance matrix \mathbf{R}_{ak}^{il} is modeled as inverse-Wishart distribution

$$p(\mathbf{R}_{ak}^{il} | \mathbf{z}_{1:k-1}) = IW(\mathbf{R}_{ak}^{il}; u_{ak|k-1}^{il}, \mathbf{U}_{ak|k-1}^{il}), \quad l \in l_k^{i*} \quad (8)$$

and $u_{ak|k-1}^{il}$ and $\mathbf{U}_{ak|k-1}^{il}$ denote the degrees of freedom (DoFs) parameter and scale matrix of $p(\mathbf{R}_{ak}^{il} | \mathbf{z}_{1:k-1})$, respectively.

In practical DCL for multirobot systems, the working environment of an exteroceptive sensor is often slowly time-varying. For example, the distance between the camera and the measured target is a slowly time-varying quantity because of the slow robot movement speed. As a result, the absolute measurement noise covariance matrix \mathbf{R}_{ak}^{il} , which depends on the distance between the camera and the measured target, is also a slowly time-varying parameter. Motivated by this fact, $u_{ak|k-1}^{il}$ and $\mathbf{U}_{ak|k-1}^{il}$ can be approximately obtained via the following linear propagation model [38]:

$$u_{ak|k-1}^{il} = \rho u_{ak-1|k-1}^{il}, \quad \mathbf{U}_{ak|k-1}^{il} = \rho \mathbf{U}_{ak-1|k-1}^{il} \quad (9)$$

where $u_{ak-1|k-1}^{il}$ and $\mathbf{U}_{ak-1|k-1}^{il}$ denote the DoF parameter and scale matrix of $p(\mathbf{R}_{ak-1}^{il} | \mathbf{z}_{1:k-1})$, respectively, and $\rho \in (0, 1]$ denotes the forgetting factor. Such linear propagation guarantees that $p(\mathbf{R}_{ak}^{il} | \mathbf{z}_{1:k-1})$ has the same mean value but increased variance (uncertainty) as compared with $p(\mathbf{R}_{ak-1}^{il} | \mathbf{z}_{1:k-1})$, which accounts for the slow time-variation and unavailable evolution model of \mathbf{R}_{ak}^{il} .

According to the relative measurement model in (5), the relative measurement likelihood PDF of robots i and j can be written as

$$p(\mathbf{z}_{rk}^{ij} | \mathbf{x}_k^i, \mathbf{x}_k^j, \mathbf{R}_{rk}^{ij}) = N(\mathbf{z}_{rk}^{ij}; \mathbf{h}_{rk}^{ij}(\mathbf{x}_k^i, \mathbf{x}_k^j), \mathbf{R}_{rk}^{ij}), \quad j \in j_k^{i*} \quad (10)$$

where the relative measurement noise covariance matrix \mathbf{R}_{rk}^{ij} is assumed as a random variable and modeled as inverse-Wishart distribution

$$p(\mathbf{R}_{rk}^{ij} | \mathbf{z}_{1:k-1}, \{\mathbf{z}_{ak}^{il}\}_{l \in l_k^{i*}}) = IW(\mathbf{R}_{rk}^{ij}; u_{rk|k-1}^{ij}, \mathbf{U}_{rk|k-1}^{ij}), \quad j \in j_k^{i*} \quad (11)$$

and $u_{rk|k-1}^{ij}$ and $\mathbf{U}_{rk|k-1}^{ij}$ denote the DoF parameter and scale matrix of $p(\mathbf{R}_{rk}^{ij} | \mathbf{z}_{1:k-1}, \{\mathbf{z}_{ak}^{il}\}_{l \in l_k^{i*}})$, respectively, which can be obtained using a similar way to (9) as follows:

$$u_{rk|k-1}^{ij} = \rho u_{rk-1|k-1}^{ij}, \quad \mathbf{U}_{rk|k-1}^{ij} = \rho \mathbf{U}_{rk-1|k-1}^{ij} \quad (12)$$

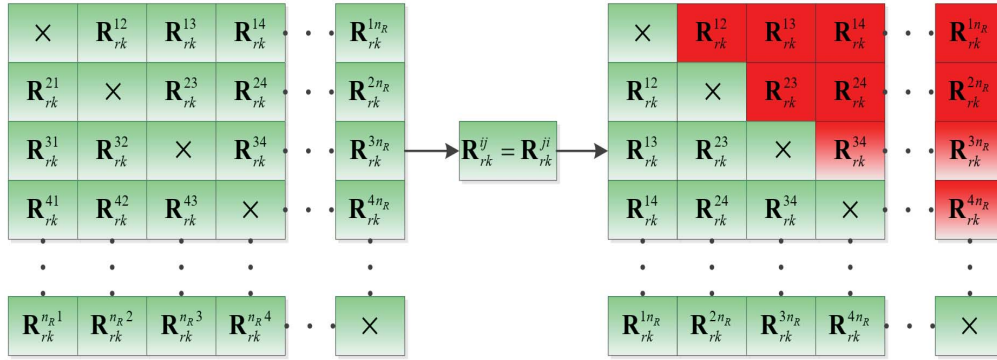


Fig. 3. All relative measurement noise covariance matrices for the entire system.

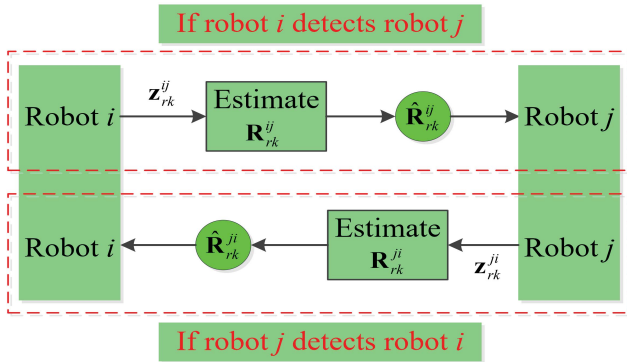


Fig. 4. Diagram of the proposed decentralized estimation strategy for $\{\mathbf{R}_{rk}^{ij}, \mathbf{R}_{rk}^{ji}\}$.

where $u_{rk-1|k-1}^{ij}$ and $\mathbf{U}_{rk-1|k-1}^{ij}$ denote the DoF parameter and scale matrix of $p(\mathbf{R}_{rk-1}^{ij} | \mathbf{z}_{1:k-1})$, respectively. It is noted that the absolute measurements $\{\mathbf{z}_{ak}^{il}\}_{l \in I_k^{i*}}$ have been obtained when \mathbf{R}_{rk}^{ij} is adaptively estimated.

Equations (6)–(12) make up an hierarchical Gaussian model of robot i whose graphical illustration is shown in Fig. 6. Using a similar way, n_R hierarchical Gaussian models of the entire multirobot systems can be constructed. Next, we will present how to jointly estimate the state vector (pose) of robot i and measurement noise covariance matrices based on these n_R hierarchical Gaussian models using the VB approach.

C. Joint Estimates of \mathbf{x}_k^i and $\{\mathbf{R}_{ak}^{il}\}_{l \in I_k^{i*}}$

To estimate \mathbf{x}_k^i and $\{\hat{\mathbf{R}}_{ak}^{il}\}_{l \in I_k^{i*}}$ simultaneously, we require to calculate the joint posterior PDF $p(\mathbf{x}_k^i, \{\hat{\mathbf{R}}_{ak}^{il}\}_{l \in I_k^{i*}} | \mathbf{z}_{1:k-1}, \{\mathbf{z}_{ak}^{il}\}_{l \in I_k^{i*}})$. Unfortunately, a recursive analytical solution of this joint posterior PDF is unavailable since the Gaussian-inverse-Wishart joint PDF does not have a closed form under the Bayesian estimation framework. To solve this problem, the standard VB approach [40], [41] is employed to obtain a free factored approximation of the joint posterior PDF as follows:

$$p(\mathbf{x}_k^i, \{\hat{\mathbf{R}}_{ak}^{il}\}_{l \in I_k^{i*}} | \mathbf{z}_{1:k-1}, \{\mathbf{z}_{ak}^{il}\}_{l \in I_k^{i*}}) \approx q^{(a)}(\mathbf{x}_k^i) \prod_{l \in I_k^{i*}} q^{(a)}(\mathbf{R}_{ak}^{il}) \quad (13)$$

where $q^{(a)}(\mathbf{x}_k^i)$ and $\{q^{(a)}(\mathbf{R}_{ak}^{il})\}_{l \in I_k^{i*}}$ are the approximate posterior PDFs of the LAMU, which are given by

$$\log q^{(a)}(\mathbf{x}_k^i) = \mathbb{E}_{\{\hat{\mathbf{R}}_{ak}^{il}\}_{l \in I_k^{i*}}} \left[\log p(\mathbf{x}_k^i, \{\hat{\mathbf{R}}_{ak}^{il}\}_{l \in I_k^{i*}}, \mathbf{z}_{1:k-1}, \{\mathbf{z}_{ak}^{il}\}_{l \in I_k^{i*}}) \right] \quad (14)$$

$$\log q^{(a)}(\mathbf{R}_{ak}^{il}) = \mathbb{E}_{\{\mathbf{x}_k^i, \{\hat{\mathbf{R}}_{ak}^{is}\}_{s \in I_k^{i*}}\}} \left[\log p(\mathbf{x}_k^i, \{\hat{\mathbf{R}}_{ak}^{il}\}_{l \in I_k^{i*}}, \mathbf{z}_{1:k-1}, \{\mathbf{z}_{ak}^{il}\}_{l \in I_k^{i*}}) \right] \quad (15)$$

where $\mathbb{E}_y[\cdot]$ denotes the expectation operation with respect to the approximate posterior PDF $q(y)$.

Proposition 1: Exploiting (14), the approximate posterior PDF $q^{(a)}(\mathbf{x}_k^i)$ can be updated as Gaussian, that is

$$q^{(a)}(\mathbf{x}_k^i) = \mathcal{N}(\mathbf{x}_k^i; \hat{\mathbf{x}}_{k|k}^{i(a)}, \boldsymbol{\Sigma}_{k|k}^{i(a)}) \quad (16)$$

where $\hat{\mathbf{x}}_{k|k}^{i(a)}$ and $\boldsymbol{\Sigma}_{k|k}^{i(a)}$ can be obtained by running the LAMU function with $\{\mathbf{z}_{ak}^{il}, \hat{\mathbf{R}}_{ak}^{il}, \mathbf{x}_L^i\}_{l \in I_k^{i*}}$, and $\hat{\mathbf{R}}_{ak}^{il}$ denotes the estimated absolute measurement noise covariance matrix and is given by

$$\hat{\mathbf{R}}_{ak}^{il} = \left\{ \mathbb{E} \left[(\mathbf{R}_{ak}^{il})^{-1} \right] \right\}^{-1}, \quad l \in I_k^{i*}. \quad (17)$$

Proposition 2: Using (15), the approximate posterior PDF $q^{(a)}(\mathbf{R}_{ak}^{il})$ can be updated as an inverse-Wishart PDF, that is

$$q^{(a)}(\mathbf{R}_{ak}^{il}) = \text{IW}(\mathbf{R}_{ak}^{il}; u_{ak|k}^{il}, \mathbf{U}_{ak|k}^{il}) \quad (18)$$

where the posterior DoF parameter $u_{ak|k}^{il}$ and scale matrix $\mathbf{U}_{ak|k}^{il}$ are, respectively, given by

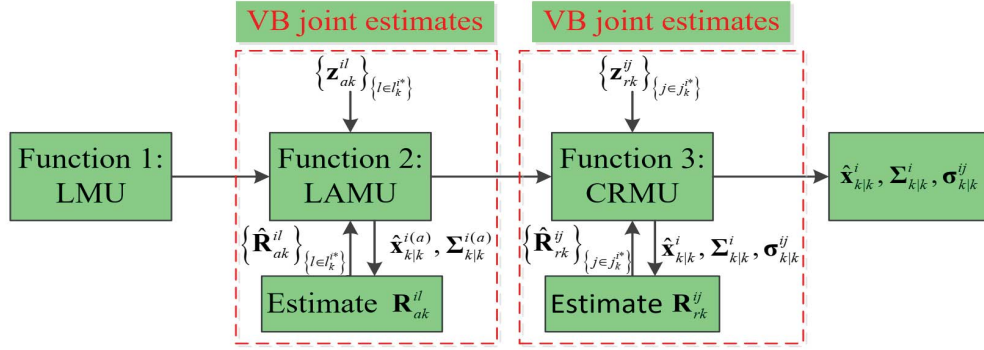
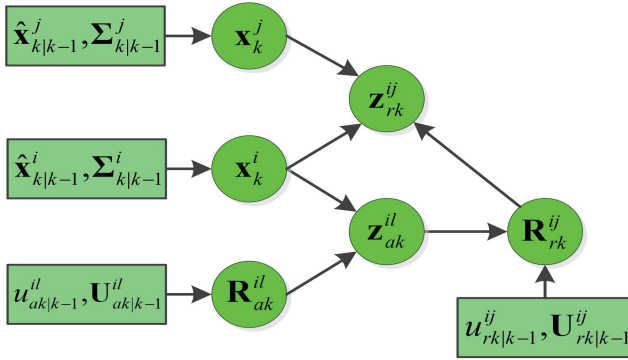
$$\begin{cases} u_{ak|k}^{il} = u_{ak|k-1}^{il} + 1 \\ \mathbf{U}_{ak|k}^{il} = \mathbf{U}_{ak|k-1}^{il} + \mathbf{A}_k^{il} \end{cases} \quad (19)$$

and the auxiliary matrix \mathbf{A}_k^{il} is written as

$$\mathbf{A}_k^{il} = \mathbb{E} \left[[\mathbf{z}_{ak}^{il} - \mathbf{h}_{ak}^{il}(\mathbf{x}_k^i, \mathbf{x}_L^i)] [\mathbf{z}_{ak}^{il} - \mathbf{h}_{ak}^{il}(\mathbf{x}_k^i, \mathbf{x}_L^i)]^T \right]. \quad (20)$$

Proof: See Appendix A for the proofs of Propositions 1 and 2. \square

Finally, we calculate the required expectations in (17) and (20). Since the scale matrix \mathbf{R}_{ak}^{il} is updated as an


 Fig. 5. Diagram of the proposed RDCL-EKF method for robot i .

 Fig. 6. Graphical illustration of the constructed hierarchical Gaussian model for robot i .

inverse-Wishart PDF according to (18), the estimate of \mathbf{R}_{ak}^{il} is calculated as

$$\hat{\mathbf{R}}_{ak}^{il} = \left\{ \mathbb{E} \left[\left(\mathbf{R}_{ak}^{il} \right)^{-1} \right] \right\}^{-1} = \mathbf{U}_{ak|k}^{il} / u_{ak|k}^{il}. \quad (21)$$

Utilizing the first-order Taylor approximation of $\mathbf{h}_{ak}^{il}(\mathbf{x}_k^i, \mathbf{x}_L^i)$ at $\hat{\mathbf{x}}_k^i = \hat{\mathbf{x}}_{k|k-1}^i$, the auxiliary matrix \mathbf{A}_k^{il} can be approximately calculated as

$$\begin{aligned} \mathbf{A}_k^{il} &= \mathbb{E} \left\{ \left[\mathbf{z}_{ak}^{il} - \mathbf{h}_{ak}^{il}(\hat{\mathbf{x}}_{k|k-1}^i, \mathbf{x}_L^i) - \mathbf{H}_{ak}^{il}(\mathbf{x}_k^i - \hat{\mathbf{x}}_{k|k-1}^i) \right] \right. \\ &\quad \left. \left[\mathbf{z}_{ak}^{il} - \mathbf{h}_{ak}^{il}(\hat{\mathbf{x}}_{k|k-1}^i, \mathbf{x}_L^i) \right. \right. \\ &\quad \left. \left. - \mathbf{H}_{ak}^{il}(\mathbf{x}_k^i - \hat{\mathbf{x}}_{k|k-1}^i) \right]^T \right\} \\ &= \mathbf{H}_{ak}^{il} \Sigma_{k|k}^{i(a)} \left(\mathbf{H}_{ak}^{il} \right)^T \\ &\quad + \left[\mathbf{z}_{ak}^{il} - \mathbf{h}_{ak}^{il}(\hat{\mathbf{x}}_{k|k-1}^i, \mathbf{x}_L^i) - \mathbf{H}_{ak}^{il}(\hat{\mathbf{x}}_{k|k}^{i(a)} - \hat{\mathbf{x}}_{k|k-1}^i) \right] \\ &\quad \times \left[\mathbf{z}_{ak}^{il} - \mathbf{h}_{ak}^{il}(\hat{\mathbf{x}}_{k|k-1}^i, \mathbf{x}_L^i) - \mathbf{H}_{ak}^{il}(\hat{\mathbf{x}}_{k|k}^{i(a)} - \hat{\mathbf{x}}_{k|k-1}^i) \right]^T \end{aligned} \quad (22)$$

where \mathbf{H}_{ak}^{il} is given in Table II.

Equations (16)–(22) constitute the proposed VB-based LAMU. It can be seen from (16) to (22) that the calculations of the approximate posterior PDFs $q^{(a)}(\mathbf{x}_k^i)$ and $\{q^{(a)}(\mathbf{R}_{ak}^{il})\}_{l \in I_k^{i*}}$ are mutually coupled. As a result, the analytical solutions of these approximate posterior PDFs are unavailable. To address this problem, in this article, the fixed-point iteration method is employed to achieve approximate solutions of these posterior PDFs, in which the posterior PDFs $q^{(a)}(\mathbf{x}_k^i)$ and

$\{q^{(a)}(\mathbf{R}_{ak}^{il})\}_{l \in I_k^{i*}}$ are alternately updated. That is to say, at the $(m+1)$ th iteration, the posterior PDF $q^{(a)}(\mathbf{x}_k^i)$ is first updated as $q^{(a)(m+1)}(\mathbf{x}_k^i)$ by fixing $\{q^{(a)}(\mathbf{R}_{ak}^{il}) = q^{(a)(m)}(\mathbf{R}_{ak}^{il})\}_{l \in I_k^{i*}}$, and then the posterior PDFs $\{q^{(a)}(\mathbf{R}_{ak}^{il})\}_{l \in I_k^{i*}}$ are updated as $\{q^{(a)(m+1)}(\mathbf{R}_{ak}^{il})\}_{l \in I_k^{i*}}$ based on the updated posterior PDF $q^{(a)(m+1)}(\mathbf{x}_k^i)$. Such fixed-point iterations are performed until convergence in the proposed VB-based LAMU. The fixed-point iteration of the proposed VB-based LAMU for robot i is summarized as the VBLAMU function in Table IV, where m^* , M and ϵ denote the actual number of iterations, the maximum number of iterations, and the iterative threshold, respectively.

D. Joint Estimates of \mathbf{x}_k^i , $\{\mathbf{x}_k^j\}_{j \in J_k^{i*}}$ and $\{\mathbf{R}_{rk}^{ij}\}_{j \in J_k^{i*}}$

To jointly estimate \mathbf{x}_k^i , $\{\mathbf{x}_k^j\}_{j \in J_k^{i*}}$ and $\{\mathbf{R}_{rk}^{ij}\}_{j \in J_k^{i*}}$, we need to calculate the joint posterior PDF $p(\mathbf{x}_k^i, \{\mathbf{x}_k^j\}_{j \in J_k^{i*}}, \{\mathbf{R}_{rk}^{ij}\}_{j \in J_k^{i*}} | \mathbf{z}_{1:k-1}, \{\mathbf{z}_{ak}^{il}\}_{l \in I_k^{i*}}, \{\mathbf{z}_{rk}^{ij}\}_{j \in J_k^{i*}})$. Similar to Section III-C, we also employ the standard VB approach [41] to obtain a free-factored approximate solution of this joint posterior PDF as follows:

$$\begin{aligned} p \left(\mathbf{x}_k^i, \{\mathbf{x}_k^j\}_{j \in J_k^{i*}}, \{\mathbf{R}_{rk}^{ij}\}_{j \in J_k^{i*}} | \mathbf{z}_{1:k-1}, \{\mathbf{z}_{ak}^{il}\}_{l \in I_k^{i*}}, \{\mathbf{z}_{rk}^{ij}\}_{j \in J_k^{i*}} \right) \\ \approx q \left(\mathbf{x}_k^i, \{\mathbf{x}_k^j\}_{j \in J_k^{i*}} \right) \times \prod_{j \in J_k^{i*}} q \left(\mathbf{R}_{rk}^{ij} \right) \end{aligned} \quad (23)$$

where $q(\mathbf{x}_k^i, \{\mathbf{x}_k^j\}_{j \in J_k^{i*}})$ and $q(\mathbf{R}_{rk}^{ij})_{j \in J_k^{i*}}$ are the approximate posterior PDFs of the CRMU, which are given by

$$\begin{aligned} \log q \left(\mathbf{x}_k^i, \{\mathbf{x}_k^j\}_{j \in J_k^{i*}} \right) \\ = \mathbb{E}_{\{\mathbf{R}_{rk}^{ij}\}_{j \in J_k^{i*}}} \left[\log p \left(\mathbf{x}_k^i, \{\mathbf{x}_k^j\}_{j \in J_k^{i*}}, \{\mathbf{R}_{rk}^{ij}\}_{j \in J_k^{i*}}, \mathbf{z}_{1:k-1}, \right. \right. \\ \left. \left. \{\mathbf{z}_{ak}^{il}\}_{l \in I_k^{i*}}, \{\mathbf{z}_{rk}^{ij}\}_{j \in J_k^{i*}} \right) \right] \end{aligned} \quad (24)$$

$$\begin{aligned} \log q \left(\mathbf{R}_{rk}^{ij} \right) \\ = \mathbb{E}_{\left\{ \mathbf{x}_k^i, \{\mathbf{x}_k^j\}_{j \in J_k^{i*}}, \{\mathbf{R}_{rk}^{is}\}_{s \in J_k^{i*}} \right\}} \left[\log p \left(\mathbf{x}_k^i, \{\mathbf{x}_k^j\}_{j \in J_k^{i*}}, \right. \right. \\ \left. \left. \{\mathbf{R}_{rk}^{ij}\}_{j \in J_k^{i*}}, \mathbf{z}_{1:k-1}, \{\mathbf{z}_{ak}^{il}\}_{l \in I_k^{i*}}, \{\mathbf{z}_{rk}^{ij}\}_{j \in J_k^{i*}} \right) \right]. \end{aligned} \quad (25)$$

TABLE IV
FIXED-POINT ITERATION OF THE PROPOSED VB-BASED LAMU FOR ROBOT i

Function 4: $\left(\hat{\mathbf{x}}_{k|k}^{i(a)}, \Sigma_{k|k}^{i(a)}, \left\{ \sigma_{k|k}^{ij(a)} \right\}, \left\{ u_{ak|k}^{il}, \mathbf{U}_{ak|k}^{il} \right\}_{\{l \in l_k^{i*}\}} \right) = \text{VBLAMU} \left(\hat{\mathbf{x}}_{k|k-1}^i, \Sigma_{k|k-1}^i, \left\{ \sigma_{k|k-1}^{ij} \right\}_{\{1 \leq j \leq n_R\}}^{\{j \neq i\}}, l_k^{i*}, \left\{ \mathbf{z}_{ak}^{il}, u_{ak|k-1}^{il}, \mathbf{U}_{ak|k-1}^{il}, \mathbf{x}_L^l \right\}_{\{l \in l_k^{i*}\}}, M, \epsilon \right)$

If the detected landmark set l_k^{i*} of robot i is non-empty:

1. Initialization: $u_{ak|k}^{il(0)} = u_{ak|k-1}^{il}$, $\mathbf{U}_{ak|k}^{il(0)} = \mathbf{U}_{ak|k-1}^{il}$, $\hat{\mathbf{R}}_{ak}^{il(0)} = \mathbf{U}_{ak|k}^{il(0)} / u_{ak|k}^{il(0)}$ for all $l \in l_k^{i*}$

2. Fixed-point iteration:

for $m = 0 : M - 1$ **do**

Update posterior PDF $q^{(a)(m+1)}(\mathbf{x}_k^i)$

Run $\left(\hat{\mathbf{x}}_{k|k}^{i(a)(m+1)}, \Sigma_{k|k}^{i(a)(m+1)}, \left\{ \sigma_{k|k}^{ij(a)(m+1)} \right\}_{\{1 \leq j \leq n_R\}}^{\{j \neq i\}}, \left\{ \mathbf{z}_{ak}^{il}, \hat{\mathbf{R}}_{ak}^{il(m)}, \mathbf{x}_L^l \right\}_{\{l \in l_k^{i*}\}} \right) = \text{LAMU} \left(\hat{\mathbf{x}}_{k|k-1}^i, \Sigma_{k|k-1}^i, \left\{ \sigma_{k|k-1}^{ij} \right\}_{\{1 \leq j \leq n_R\}}^{\{j \neq i\}}, l_k^{i*}, \left\{ \mathbf{z}_{ak}^{il}, \hat{\mathbf{R}}_{ak}^{il(m)}, \mathbf{x}_L^l \right\}_{\{l \in l_k^{i*}\}} \right)$

Calculate $\mathbf{A}_k^{il(m+1)} = \mathbf{H}_{ak}^{il} \Sigma_{k|k}^{i(a)(m+1)} (\mathbf{H}_{ak}^{il})^T + \left[\mathbf{z}_{ak}^{il} - \mathbf{h}_{ak}^{il}(\hat{\mathbf{x}}_{k|k-1}^i, \mathbf{x}_L^l) - \mathbf{H}_{ak}^{il}(\hat{\mathbf{x}}_{k|k}^{i(a)(m+1)} - \hat{\mathbf{x}}_{k|k-1}^i) \right] \times \left[\mathbf{z}_{ak}^{il} - \mathbf{h}_{ak}^{il}(\hat{\mathbf{x}}_{k|k-1}^i, \mathbf{x}_L^l) - \mathbf{H}_{ak}^{il}(\hat{\mathbf{x}}_{k|k}^{i(a)(m+1)} - \hat{\mathbf{x}}_{k|k-1}^i) \right]^T$

Update posterior PDFs $q^{(a)(m+1)}(\mathbf{R}_{ak}^{il})$

Calculate $u_{ak|k}^{il(m+1)} = u_{ak|k-1}^{il} + 1$, $\mathbf{U}_{ak|k}^{il(m+1)} = \mathbf{U}_{ak|k-1}^{il} + \mathbf{A}_k^{il(m+1)}$, $\hat{\mathbf{R}}_{ak}^{il(m+1)} = \mathbf{U}_{ak|k}^{il(m+1)} / u_{ak|k}^{il(m+1)}$

Check convergence: if $\frac{\|\hat{\mathbf{x}}_{k|k}^{i(a)(m+1)} - \hat{\mathbf{x}}_{k|k}^{i(a)(m)}\|}{\|\hat{\mathbf{x}}_{k|k}^{i(a)(m+1)}\|} \leq \epsilon$, terminate iteration

end for

3. Save $\hat{\mathbf{x}}_{k|k}^{i(a)} = \hat{\mathbf{x}}_{k|k}^{i(a)(m^*)}$, $\Sigma_{k|k}^{i(a)} = \Sigma_{k|k}^{i(a)(m^*)}$, $\left\{ \sigma_{k|k}^{ij(a)} = \sigma_{k|k}^{ij(a)(m^*)} \right\}_{\{1 \leq j \leq n_R\}}^{\{j \neq i\}}$, $\left\{ u_{ak|k}^{il} = u_{ak|k}^{il(m^*)}, \mathbf{U}_{ak|k}^{il} = \mathbf{U}_{ak|k}^{il(m^*)} \right\}_{\{l \in l_k^{i*}\}}$

If the detected landmark set l_k^{i*} of robot i is empty: $\hat{\mathbf{x}}_{k|k}^{i(a)} = \hat{\mathbf{x}}_{k|k-1}^i$, $\Sigma_{k|k}^{i(a)} = \Sigma_{k|k-1}^i$, $\left\{ \sigma_{k|k}^{ij(a)} = \sigma_{k|k-1}^{ij} \right\}_{\{1 \leq j \leq n_R\}}^{\{j \neq i\}}$

$\left\{ u_{ak|k}^{il} = u_{ak|k-1}^{il}, \mathbf{U}_{ak|k}^{il} = \mathbf{U}_{ak|k-1}^{il} \right\}_{\{l \in l_k^{i*}\}}$

Proposition 3: Exploiting (24), the approximate posterior PDF $q(\mathbf{x}_k^i, \{\mathbf{x}_k^j\}_{\{j \in j_k^{i*}\}})$ can be updated as Gaussian, that is

$$q\left(\mathbf{x}_k^i, \left\{ \mathbf{x}_k^j \right\}_{\{j \in j_k^{i*}\}}\right) = \mathcal{N}\left(\begin{bmatrix} \mathbf{x}_k^i \\ \mathbf{x}_k^j \end{bmatrix}; \begin{bmatrix} \hat{\mathbf{x}}_{k|k}^i \\ \hat{\mathbf{x}}_{k|k}^j \end{bmatrix}, \begin{bmatrix} \Sigma_{k|k}^i & \Sigma_{k|k}^{ij*} \\ (\Sigma_{k|k}^i)^T & \Sigma_{k|k}^j \end{bmatrix}\right) \quad (26)$$

where the state estimates $\hat{\mathbf{x}}_{k|k}^i$ and $\hat{\mathbf{x}}_{k|k}^{j*}$, the estimation error covariance matrix $\Sigma_{k|k}^i$ and $\Sigma_{k|k}^{ij*}$, and the cross correlation $\Sigma_{k|k}^{jk*}$ can be obtained using the CRMU function with $\{\mathbf{z}_{rk}^{ij}, \hat{\mathbf{R}}_{rk}^{ij}\}_{\{j \in j_k^{i*}\}}$, and the estimated relative measurement noise covariance matrix $\hat{\mathbf{R}}_{rk}^{ij}$ is written as

$$\hat{\mathbf{R}}_{rk}^{ij} = \left\{ \mathbb{E} \left[\left(\mathbf{R}_{rk}^{ij} \right)^{-1} \right] \right\}^{-1}. \quad (27)$$

Proposition 4: According to (25), the approximate posterior PDF $q(\mathbf{R}_{rk}^{ij})$ can be updated as an inverse-Wishart PDF as follows:

$$q\left(\mathbf{R}_{rk}^{ij}\right) = \text{IW}\left(\mathbf{R}_{rk}^{ij}; u_{rk|k}^{ij}, \mathbf{U}_{rk|k}^{ij}\right) \quad (28)$$

where the posterior DoF parameter $u_{rk|k}^{ij}$ and scale matrix $\mathbf{U}_{rk|k}^{ij}$ are, respectively, given by

$$\begin{cases} u_{rk|k}^{ij} = u_{rk|k-1}^{ij} + 1 \\ \mathbf{U}_{rk|k}^{ij} = \mathbf{U}_{rk|k-1}^{ij} + \mathbf{B}_k^{ij} \end{cases} \quad (29)$$

and the auxiliary matrix \mathbf{B}_k^{ij} is formulated as

$$\mathbf{B}_k^{ij} = \mathbb{E} \left\{ \left[\mathbf{z}_{rk}^{ij} - \mathbf{h}_{rk}^{ij}(\mathbf{x}_k^i, \mathbf{x}_k^j) \right] \left[\mathbf{z}_{rk}^{ij} - \mathbf{h}_{rk}^{ij}(\mathbf{x}_k^i, \mathbf{x}_k^j) \right]^T \right\} \quad (30)$$

Proof: See Appendix B for the proofs of Propositions 3 and 4. \square

Similar to Section III-C, the expectations in (27) and (30) can be, respectively, calculated as

$$\hat{\mathbf{R}}_{rk}^{ij} = \mathbf{U}_{rk|k}^{ij} / u_{rk|k}^{ij} \quad (31)$$

$$\begin{aligned} \mathbf{B}_k^{ij} &= \mathbf{H}_{rk}^{ij} \Sigma_{k|k}^{ij*} (\mathbf{H}_{rk}^{ij})^T \\ &+ \left[\mathbf{z}_{rk}^{ij} - \mathbf{h}_{rk}^{ij}(\hat{\mathbf{x}}_{k|k}^i, \hat{\mathbf{x}}_{k|k}^j) - \mathbf{H}_{rk}^{ij}(\xi_{k|k}^{ij} - \xi_{k|k}^{ij(a)}) \right] \\ &\times \left[\mathbf{z}_{rk}^{ij} - \mathbf{h}_{rk}^{ij}(\hat{\mathbf{x}}_{k|k}^i, \hat{\mathbf{x}}_{k|k}^j) - \mathbf{H}_{rk}^{ij}(\xi_{k|k}^{ij} - \xi_{k|k}^{ij(a)}) \right]^T \end{aligned} \quad (32)$$

TABLE V
FIXED-POINT ITERATION OF THE PROPOSED VB-BASED CRMU FOR ROBOT i

Function 5: $\left(\hat{\mathbf{x}}_{k|k}^i, \Sigma_{k|k}^i, \left\{ \sigma_{k|k}^{ij} \right\}_{\{j \neq i\}}^{\{1 \leq j \leq n_R\}}, \left\{ u_{rk|k}^{ij}, \mathbf{U}_{rk|k}^{ij} \right\}_{\{j \in j_k^{i*}\}} \right) = \text{VBCRMU} \left(\hat{\mathbf{x}}_{k|k}^{i(a)}, \Sigma_{k|k}^{i(a)}, \left\{ \sigma_{k|k}^{ij(a)} \right\}_{\{1 \leq j \leq n_R\}}^{\{j \neq i\}}, j_k^{i*}, \left\{ \mathbf{z}_{rk}^{ij}, u_{rk|k-1}^{ij}, \mathbf{U}_{rk|k-1}^{ij} \right\}_{\{j \in j_k^{i*}\}}, M, \epsilon \right)$

If the detected robot set j_k^{i*} of robot i is non-empty:

1. Initialization: $u_{rk|k}^{ij(0)} = u_{rk|k-1}^{ij}, \mathbf{U}_{rk|k}^{ij(0)} = \mathbf{U}_{rk|k-1}^{ij}, \hat{\mathbf{R}}_{rk}^{ij(0)} = \mathbf{U}_{rk|k}^{ij(0)} / u_{rk|k}^{ij(0)}$ for all $j \in j_k^{i*}$
2. Fixed-point iteration:

for $m = 0 : M - 1$ **do**

Update posterior PDF $q^{(m+1)}(\mathbf{x}_k^i, \{\mathbf{x}_k^j\}_{\{j \in j_k^{i*}\}})$

Run $\left(\hat{\mathbf{x}}_{k|k}^{i(m+1)}, \Sigma_{k|k}^{i(m+1)}, \left\{ \sigma_{k|k}^{ij(m+1)} \right\}_{\{j \neq i\}}^{\{1 \leq j \leq n_R\}} \right) = \text{CRMU} \left(\hat{\mathbf{x}}_{k|k}^{i(a)}, \Sigma_{k|k}^{i(a)}, \left\{ \sigma_{k|k}^{ij(a)} \right\}_{\{1 \leq j \leq n_R\}}^{\{j \neq i\}}, j_k^{i*}, \left\{ \mathbf{z}_{rk}^{ij}, \hat{\mathbf{R}}_{rk}^{ij(m)} \right\}_{\{j \in j_k^{i*}\}} \right)$

Save $\hat{\mathbf{x}}_{k|k}^{j_k^{i*}(m+1)}, \Sigma_{k|k}^{j_k^{i*}(m+1)}, \Sigma_{k|k}^{j_k^{i*}(m+1)}$ produced in the CRMU function

Extract $\hat{\mathbf{x}}_{k|k}^{ij(m+1)}, \Sigma_{k|k}^{ij(m+1)}$, and $\Sigma_{k|k}^{j(m+1)}$ from $\hat{\mathbf{x}}_{k|k}^{j_k^{i*}(m+1)}, \Sigma_{k|k}^{j_k^{i*}(m+1)}, \Sigma_{k|k}^{j_k^{i*}(m+1)}$, respectively.

Construct $\Sigma_{k|k}^{\xi^{ij} \xi^{ij(m+1)}} = \begin{bmatrix} \Sigma_{k|k}^{i(m+1)} & \Sigma_{k|k}^{ij(m+1)} \\ \left(\Sigma_{k|k}^{ij(m+1)} \right)^T & \Sigma_{k|k}^{j(m+1)} \end{bmatrix}, \xi_{k|k}^{ij(m+1)} = \begin{bmatrix} \hat{\mathbf{x}}_{k|k}^{i(m+1)} \\ \hat{\mathbf{x}}_{k|k}^{j(m+1)} \end{bmatrix}, \xi_{k|k}^{ij(a)} = \begin{bmatrix} \hat{\mathbf{x}}_{k|k}^{i(a)} \\ \hat{\mathbf{x}}_{k|k}^{j(a)} \end{bmatrix}$

Calculate $\mathbf{B}_k^{ij(m+1)} = \mathbf{H}_{rk}^{ij} \Sigma_{k|k}^{\xi^{ij} \xi^{ij(m+1)}} \left(\mathbf{H}_{rk}^{ij} \right)^T + \left[\mathbf{z}_{rk}^{ij} - \mathbf{h}_{rk}^{ij} \left(\hat{\mathbf{x}}_{k|k}^{i(a)}, \hat{\mathbf{x}}_{k|k}^{j(a)} \right) - \mathbf{H}_{rk}^{ij} \left(\xi_{k|k}^{ij(m+1)} - \xi_{k|k}^{ij(a)} \right) \right] \times \left[\mathbf{z}_{rk}^{ij} - \mathbf{h}_{rk}^{ij} \left(\hat{\mathbf{x}}_{k|k}^{i(a)}, \hat{\mathbf{x}}_{k|k}^{j(a)} \right) - \mathbf{H}_{rk}^{ij} \left(\xi_{k|k}^{ij(m+1)} - \xi_{k|k}^{ij(a)} \right) \right]^T$

Update posterior PDFs $q^{(m+1)}(\mathbf{R}_{rk}^{ij})$ for all $j \in j_k^{i*}$

Calculate $u_{rk|k}^{ij(m+1)} = u_{rk|k-1}^{ij} + 1, \mathbf{U}_{rk|k}^{ij(m+1)} = \mathbf{U}_{rk|k-1}^{ij} + \mathbf{B}_k^{ij(m+1)}, \hat{\mathbf{R}}_{rk}^{ij(m+1)} = \mathbf{U}_{rk|k}^{ij(m+1)} / u_{rk|k}^{ij(m+1)}$

Check convergence: if $\frac{\|\hat{\mathbf{x}}_{k|k}^{i(m+1)} - \hat{\mathbf{x}}_{k|k}^{i(m)}\|}{\|\hat{\mathbf{x}}_{k|k}^{i(m+1)}\|} \leq \epsilon$, terminate iteration

end for
3. Save $\hat{\mathbf{x}}_{k|k}^i = \hat{\mathbf{x}}_{k|k}^{i(m^*)}, \Sigma_{k|k}^i = \Sigma_{k|k}^{i(m^*)}, \left\{ \sigma_{k|k}^{ij} = \sigma_{k|k}^{ij(m^*)} \right\}_{\{1 \leq j \leq n_R\}}^{\{j \neq i\}}, \left\{ u_{rk|k}^{ij} = u_{rk|k}^{ij(m^*)}, \mathbf{U}_{rk|k}^{ij} = \mathbf{U}_{rk|k}^{ij(m^*)} \right\}_{\{j \in j_k^{i*}\}}$

If the detected robot set j_k^{i*} of robot i is empty: $\hat{\mathbf{x}}_{k|k}^i = \hat{\mathbf{x}}_{k|k}^{i(a)}, \Sigma_{k|k}^i = \Sigma_{k|k}^{i(a)}, \left\{ \sigma_{k|k}^{ij} = \sigma_{k|k}^{ij(a)} \right\}_{\{1 \leq j \leq n_R\}}^{\{j \neq i\}}, \left\{ u_{rk|k}^{ij} = u_{rk|k-1}^{ij}, \mathbf{U}_{rk|k}^{ij} = \mathbf{U}_{rk|k-1}^{ij} \right\}_{\{j \in j_k^{i*}\}}$

where the auxiliary parameters are given by

$$\left\{ \begin{array}{l} \Sigma_{k|k}^{\xi^{ij} \xi^{ij}} = \begin{bmatrix} \Sigma_{k|k}^i & \Sigma_{k|k}^{ij} \\ \left(\Sigma_{k|k}^{ij} \right)^T & \Sigma_{k|k}^j \end{bmatrix} \\ \xi_{k|k}^{ij} = \begin{bmatrix} \hat{\mathbf{x}}_{k|k}^i \\ \hat{\mathbf{x}}_{k|k}^j \end{bmatrix}, \xi_{k|k}^{ij(a)} = \begin{bmatrix} \hat{\mathbf{x}}_{k|k}^{i(a)} \\ \hat{\mathbf{x}}_{k|k}^{j(a)} \end{bmatrix} \end{array} \right. \quad (33)$$

and $\hat{\mathbf{x}}_{k|k}^j, \hat{\mathbf{x}}_{k|k}^{j(a)}, \Sigma_{k|k}^j$ and $\Sigma_{k|k}^j$ can be, respectively, extracted from $\hat{\mathbf{x}}_{k|k}^{j_k^{i*}}, \hat{\mathbf{x}}_{k|k}^{j_k^{i*}(a)}, \Sigma_{k|k}^{j_k^{i*}}$ and $\Sigma_{k|k}^{j_k^{i*}}$ accordingly.

Equations (27)–(33) constitute the proposed VB-based CRMU. We can observe from (27) to (33) that the calculations of the approximate posterior PDFs $q(\mathbf{x}_k^i, \{\mathbf{x}_k^j\}_{\{j \in j_k^{i*}\}})$ and $\{q(\mathbf{R}_{rk}^{ij})\}_{\{j \in j_k^{i*}\}}$ are also mutually coupled so that the analytical solutions of these posterior PDFs are unavailable. Similar to the proposed VB-based LAMU, the approximate posterior

PDFs $q(\mathbf{x}_k^i, \{\mathbf{x}_k^j\}_{\{j \in j_k^{i*}\}})$ and $\{q(\mathbf{R}_{rk}^{ij})\}_{\{j \in j_k^{i*}\}}$ are also alternately updated based on the fixed-point iteration in the CRMU. The fixed-point iteration of the proposed VB-based CRMU for robot i is summarized as VBCRMU function in Table V.

E. Proposed Adaptive RDCL-EKF Algorithm

The proposed adaptive RDCL-EKF algorithm is composed of four parts: the local motion updates of all robots, the local time updates of measurement noise covariance matrices of all robots, the VB-based LAMUs of all robots, and the VB-based CRMUs of all robots. The detailed update process is as follows.

- 1) In the local motion update, each robot propagates its state estimate, estimation error covariance matrix, and cross correlations independently.

TABLE VI
IMPLEMENTATIONS OF THE PROPOSED ADAPTIVE RDCL-EKF ALGORITHM

Inputs: $\{\hat{\mathbf{x}}_{k-1|k-1}^i, \Sigma_{k-1|k-1}^i, \mathbf{Q}_k^i, l_k^{i*}, j_k^{i*}\}_{1 \leq i \leq n_R}$, $\{\sigma_{k-1|k-1}^{ij}\}_{1 \leq i, j \leq n_R}^{\{j \neq i\}}$, $\{u_{ak|k-1}^{il}, \mathbf{U}_{ak|k-1}^{il}\}_{1 \leq i \leq n_R}^{\{1 \leq l \leq n_L\}}$,
 $\{\mathbf{z}_{ak}^{il}\}_{1 \leq i \leq n_R}^{\{l \in l_k^{i*}\}}$, $\{\mathbf{x}_L^l\}_{1 \leq l \leq n_L}$, $\{u_{rk|k-1}^{ij}, \mathbf{U}_{rk|k-1}^{ij}\}_{1 \leq i, j \leq n_R}^{\{i \neq j\}}$, $\{\mathbf{z}_{rk}^{ij}\}_{1 \leq i \leq n_R}^{\{j \in j_k^{i*}\}}$, ρ, M, ϵ

Local motion updates of all robots:

For all $1 \leq i \leq n_R$, robot i runs the LMU function independently:

$$\left(\hat{\mathbf{x}}_{k|k-1}^i, \Sigma_{k|k-1}^i, \{\sigma_{k|k-1}^{ij}\}_{1 \leq j \leq n_R}^{\{j \neq i\}} \right) = \text{LMU} \left(\hat{\mathbf{x}}_{k-1|k-1}^i, \Sigma_{k-1|k-1}^i, \{\sigma_{k-1|k-1}^{ij}\}_{1 \leq j \leq n_R}^{\{j \neq i\}}, \mathbf{Q}_k^i \right)$$

Local time updates of measurement noise covariance matrices of all robots:

For all $1 \leq i \leq n_R$, robot i calculates the dof parameters and scale matrices independently:

for $l = 1 : n_L$ **do**

$$u_{ak|k-1}^{il} = \rho u_{ak-1|k-1}^{il}, \quad \mathbf{U}_{ak|k-1}^{il} = \rho \mathbf{U}_{ak-1|k-1}^{il}$$

end for

for $j = 1 : n_R$ **do**

If $j \neq i$: $u_{rk|k-1}^{ij} = \rho u_{rk-1|k-1}^{ij}, \quad \mathbf{U}_{rk|k-1}^{ij} = \rho \mathbf{U}_{rk-1|k-1}^{ij}$

end for

VB based local absolute measurement updates of all robots:

For all $1 \leq i \leq n_R$, robot i runs the VBLAMU function independently:

$$\left(\hat{\mathbf{x}}_{k|k}^{i(a)}, \Sigma_{k|k}^{i(a)}, \{\sigma_{k|k}^{ij(a)}\}, \{u_{ak|k}^{il}, \mathbf{U}_{ak|k}^{il}\}_{l \in l_k^{i*}} \right) = \text{VBLAMU} \left(\hat{\mathbf{x}}_{k|k-1}^i, \Sigma_{k|k-1}^i, \{\sigma_{k|k-1}^{ij}\}_{1 \leq j \leq n_R}^{\{j \neq i\}}, l_k^{i*}, \right. \\ \left. \{\mathbf{z}_{ak}^{il}, u_{ak|k-1}^{il}, \mathbf{U}_{ak|k-1}^{il}, \mathbf{x}_L^l\}_{l \in l_k^{i*}}, M, \epsilon \right)$$

If $l \notin l_k^{i*}$: $\{u_{ak|k}^{il} = u_{ak|k-1}^{il}, \mathbf{U}_{ak|k}^{il} = \mathbf{U}_{ak|k-1}^{il}\}_{l \notin l_k^{i*}}$

VB based cooperative relative measurement updates of all robots:

For all $1 \leq i \leq n_R$, robot i runs the VBCRMU function:

$$\left(\hat{\mathbf{x}}_{k|k}^i, \Sigma_{k|k}^i, \{\sigma_{k|k}^{ij}\}_{1 \leq j \leq n_R}^{\{j \neq i\}}, \{u_{rk|k}^{ij}, \mathbf{U}_{rk|k}^{ij}\}_{j \in j_k^{i*}} \right) = \text{VBCRMU} \left(\hat{\mathbf{x}}_{k|k-1}^i, \Sigma_{k|k-1}^i, \{\sigma_{k|k-1}^{ij(a)}\}_{1 \leq j \leq n_R}^{\{j \neq i\}}, j_k^{i*}, \right. \\ \left. \{\mathbf{z}_{rk}^{ij}, u_{rk|k-1}^{ij}, \mathbf{U}_{rk|k-1}^{ij}\}_{j \in j_k^{i*}}, M, \epsilon \right)$$

If the robot i has been detected by the robot $j \in j_k^{i*}$: send $\{u_{rk|k}^{ij} = u_{rk|k-1}^{ij}, \mathbf{U}_{rk|k}^{ij} = \mathbf{U}_{rk|k-1}^{ij}\}_{j \in j_k^{i*}}$ to robot j

Else: send $\{u_{rk|k-1}^{ij} = u_{rk|k-1}^{ij}, \mathbf{U}_{rk|k-1}^{ij} = \mathbf{U}_{rk|k-1}^{ij}\}_{j \in j_k^{i*}}$ to robot j

If $j \notin j_k^{i*}$: $\{u_{rk|k}^{ij} = u_{rk|k-1}^{ij}, \mathbf{U}_{rk|k}^{ij} = \mathbf{U}_{rk|k-1}^{ij}\}_{j \notin j_k^{i*}}$

Outputs: $\{\hat{\mathbf{x}}_{k-1|k-1}^i, \Sigma_{k-1|k-1}^i\}_{1 \leq i \leq n_R}$, $\{\sigma_{k|k}^{ij}\}_{1 \leq i, j \leq n_R}^{\{j \neq i\}}$, $\{u_{ak|k}^{il}, \mathbf{U}_{ak|k}^{il}\}_{1 \leq i \leq n_R}^{\{1 \leq l \leq n_L\}}$, $\{u_{rk|k}^{ij}, \mathbf{U}_{rk|k}^{ij}\}_{1 \leq i, j \leq n_R}^{\{i \neq j\}}$

2) In the local time updates of measurement noise covariance matrices, each robot propagates its DoF parameters and scale matrices of absolute and relative measurement noise covariance matrices with respect to all landmarks and all the other robots.

3) In the VB-based LAMU, each robot updates its state estimate, estimation error covariance matrix, cross correlations, and the DoF parameters and scale matrices of the absolute measurement noise covariance matrices relative to all detected landmarks independently, while

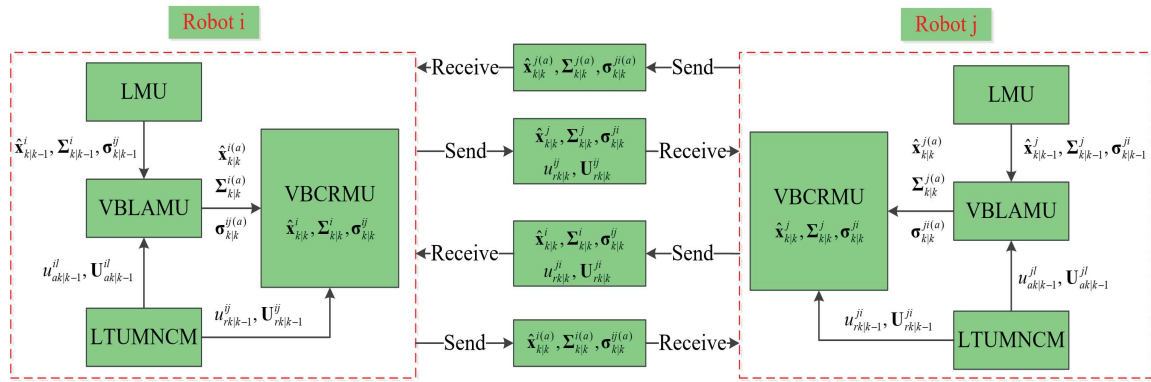


Fig. 7. Diagram of the proposed RDCL-EKF algorithm for robots i and j .

the DoF parameters and scale matrices of absolute and relative measurement noise covariance matrices relative to the undetected landmarks all remain unchanged.

- 4) In the VB-based CRMU, each robot and all the other robots detected by it jointly update their state estimates, error covariance matrices, cross correlations, and the DoF parameters and scale matrices of relative measurement noise covariance matrices.

The diagram of the proposed RDCL-EKF algorithm for robots i and j is shown in Fig. 7, where LMU, LTUMNCM, VBLAMU, and VBCRMU are, respectively, the abbreviations of the above update steps. The detailed implementations of the proposed adaptive RDCL-EKF algorithm for all robots are shown in Table VI. It can be observed from Fig. 7 that the state estimation information and the distribution parameters of the relative measurement noise covariance matrices of robot i and robot j require to interact with each other through local communication in the cooperative process between robot i and robot j . We can observe from Table VI that the proposed method does not require a common fusion center, and each robot plays a role of fusion center, in which each robot estimates its state vector (pose), absolute measurement noise covariance matrices with respect to all landmarks, and relative measurement noise covariance matrices with respect to all the other robots in a decentralized way.

Remark 1: The proposed RDCL-EKF method has the same communication mode as the existing RDCL-EKF method, but requires that the additional distribution parameters of the relative measurement noise covariance matrices are transmitted, as shown in Fig. 7. Thus, in practical CL applications, the proposed method has the same communication frequency with the existing RDCL-EKF method, but only requires slightly higher communication overhead to transmit additional parameters in each cooperation. It is worth noting that we have assumed perfect communications between the local robots, and the problems with regard to the delays and dropouts in communication will be further considered in our future work. Meanwhile, VB learning allows the robot to adaptively estimate the measurement noise covariance matrices, contributing to better performance for the problem of DCL with time-varying accuracy, but at the expense of slightly higher computational complexity.

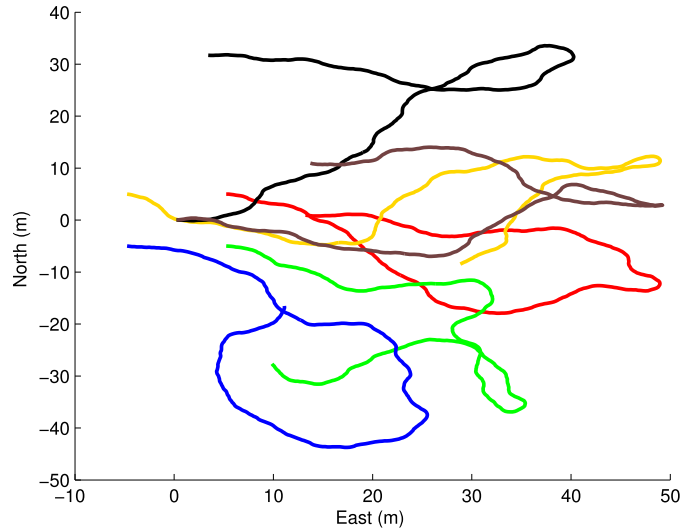


Fig. 8. True trajectories of six mobile robots.

IV. SIMULATION STUDY

A. Simulation Setups and Descriptions

In this section, the performance of the proposed adaptive RDCL-EKF algorithm is validated using a series of simulation tests. A team of six homogeneous mobile robots move randomly according to the motion model (1) in a 2-D environment with five known landmarks, that is $n_R = 6$ and $n_L = 5$, where the true linear velocity of each robot is $V_k = 0.5$ (m/s), and the true rotational velocity Ω_k of each robot is randomly drawn from $[-0.5, 0.5]$ (rad/s), and the discretization time is set as $\Delta t = 0.5$ (s). The true trajectories of six mobile robots are shown in Fig. 8. The proprioceptive sensor is selected as the wheel encoder which is used to measure the linear and rotational velocities. The wheel encoders installed on every robot have the same measurement accuracy, and the standard deviation is set as $\sigma_k = 5\%V_k$ which is proportional to the true linear velocity. According to the velocity measuring principle of wheel encoders, the standard deviations of linear and rotational velocity measurements can be, respectively, set as $\sigma_{V_k} = (\sqrt{2}/2)\sigma_k$ and $\sigma_{\Omega_k} = (\sqrt{2}/a)\sigma_k$, where a denotes the distance between two drive wheels of every robot [15].

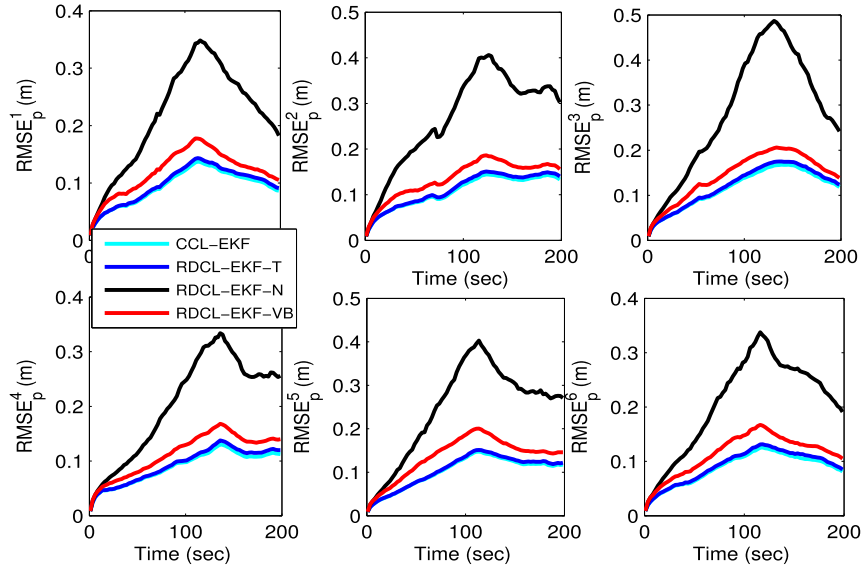


Fig. 9. RMSEs of position of all the algorithms compared for six mobile robots.

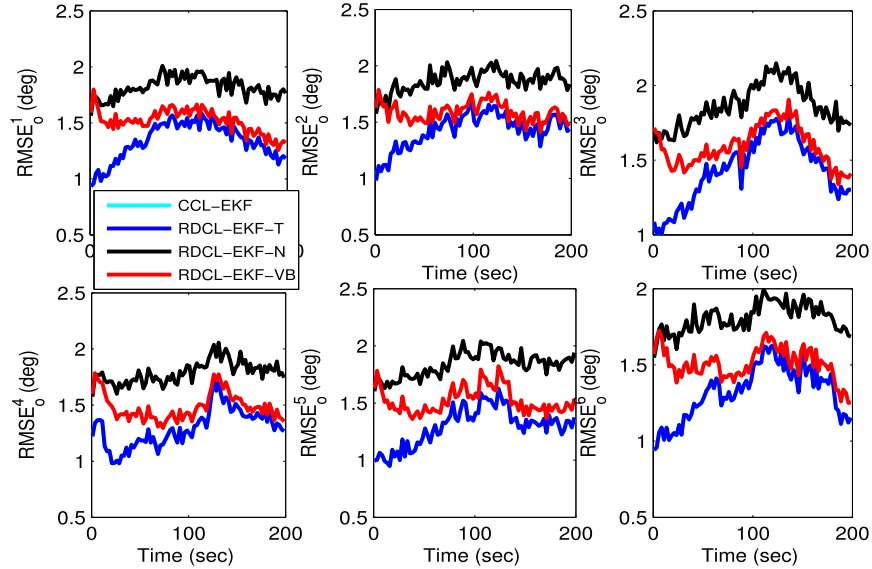


Fig. 10. RMSEs of orientation of all the algorithms compared for six mobile robots.

In this simulation study, the bearing and range measurement models in (2) and (4) are used to validate the performance of the proposed method. It is noted that the similar simulation results and conclusions can be also obtained using the relative position measurement models in (2) and (4), and they are omitted for brevity. The standard deviations of absolute measurements are all proportional to the true distance between the exteroceptive sensor and the reference landmark, and the standard deviations of relative measurements are also all proportional to the true distance between the exteroceptive sensor and the mobile robot. Considering that every exteroceptive sensor has a limiting measurement accuracy, the standard deviations of absolute and relative measurements all have the minimum values, and the minimum standard deviations of bearing and range are, respectively, chosen as 1 (deg) and 0.1 (m).

Specifically, for the absolute and relative measurements, the standard deviations of bearing and range are, respectively, set as the five percent of the distance between the exteroceptive sensor and the measured target, that is $\sigma_{\theta k} = 5\%d_k$ (deg) and $\sigma_{r k} = 5\%d_k$ (m), where $\sigma_{\theta k} \geq 1$ (deg) and $\sigma_{r k} \geq 1$ (m), and d_k denotes the true distance between the exteroceptive sensor and the measured target (reference landmark or mobile robot). Since every mobile robot has limited sensing scope, it can only detect the landmarks and other mobile robots occasionally. To be more consistent with the actual situation, it is assumed that each mobile robot detects every landmark and mobile robot both with the probability of 20%. To better show the advantages of the proposed method, four CL-EKF algorithms are compared in the simulation tests, in which the true state noise covariance matrix $\mathbf{Q}_k = \text{diag}\{\sigma_{V_k}^2, \sigma_{\Omega_r}^2\}$ of each robot

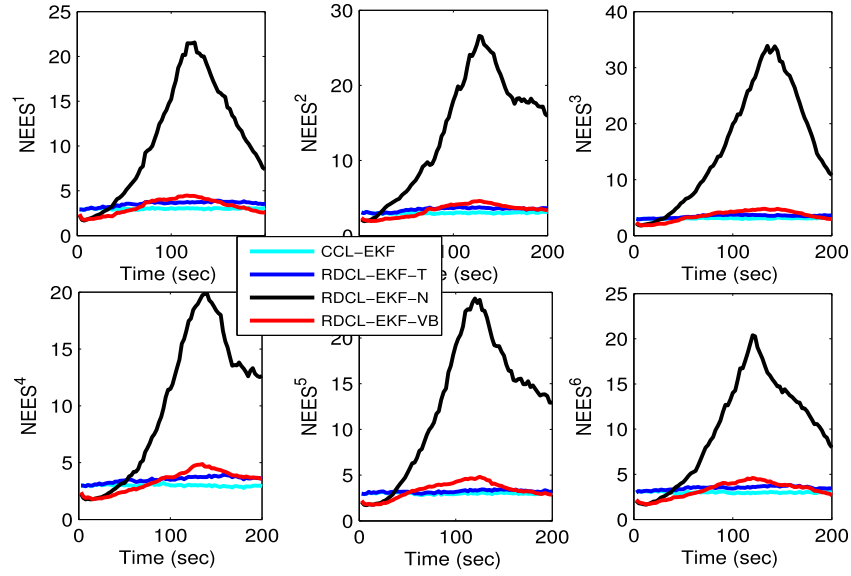


Fig. 11. NEESs of all the algorithms compared for six mobile robots.

is used. The detailed descriptions and parameter settings of the four CL-EKF algorithms are listed as follows.

- 1) *CCL-EKF* [8]: The existing CCL-EKF algorithm is the optimal centralized algorithm employing the true absolute and relative measurement noise covariance matrices \mathbf{R}_{ak} and \mathbf{R}_{rk} to estimate the poses of all robots, which is used as the most accurate reference.
- 2) *RDCL-EKF-T* [25]: The existing RDCL-EKF algorithm employs the true absolute and relative measurement noise covariance matrices \mathbf{R}_{ak} and \mathbf{R}_{rk} to estimate the poses of all robots, which acts as the benchmark for the proposed adaptive DCL method.
- 3) *RDCL-EKF-N* [25]: The existing RDCL-EKF algorithm utilizes the nominal absolute and relative measurement noise covariance matrices $\bar{\mathbf{R}}_{ak}$ and $\bar{\mathbf{R}}_{rk}$ to estimate the poses of all robots and will be compared with the proposed algorithm in terms of estimation accuracy and consistency.
- 4) *RDCL-EKF-VB*: The proposed adaptive RDCL-EKF algorithm employs the standard VB approach to estimate the absolute and relative measurement noise covariance matrices, in which the nominal absolute and relative measurement noise covariance matrices $\bar{\mathbf{R}}_{ak}$ and $\bar{\mathbf{R}}_{rk}$ are used as initial prior values, and the initial dof parameters and scale matrices are set as: $\{u_{a0|0}^{il} = 5, \mathbf{U}_{a0|0}^{il} = 5\bar{\mathbf{R}}_{a0}\}_{\{1 \leq l \leq n_L\}}$ and $\{u_{r0|0}^{ij} = 5, \mathbf{U}_{r0|0}^{ij} = 5\bar{\mathbf{R}}_{r0}\}_{\{1 \leq i, j \leq n_R\}}$, and the other parameters are selected as $\rho = 1 - 10^{-5}$, $M = 50$, $\epsilon = 10^{-4}$.

Among the above four algorithms, $\mathbf{R}_{ak} = \mathbf{R}_{rk} = \text{diag}\{\sigma_{rk}^2, \sigma_{\theta k}^2\}$ and $\bar{\mathbf{R}}_{ak} = \bar{\mathbf{R}}_{rk} = \text{diag}\{\bar{\sigma}_r^2, \bar{\sigma}_\theta^2\}$, and $\bar{\sigma}_r$ and $\bar{\sigma}_\theta$ denote the nominal standard deviations of range and bearing measurements, which are, respectively, selected as 0.5 (m) and 5 (deg). The CCL-EKF algorithm can obtain the optimal CL accuracy, and it is used as the performance benchmark for all CL-EKF algorithms. On the other hand, the RDCL-EKF-T algorithm can achieve the best CL accuracy in the RDCL-EKF

framework, and it is used as the accuracy benchmark for the RDCL-EKF-N and RDCL-EKF-VB algorithms. The codes of all algorithms are performed on a computer with Intel Core i7-6500U CPU at 2.50 GHz.

In all comparative algorithms, the initial state estimates of all robots are set as their initial true states, and the corresponding estimation error covariance matrices are all set as $10^{-10}\mathbf{I}$. Simulation time is set as 200 (s) and 1000 Monte Carlo run simulation trials are performed. To compare the CL accuracy, the root mean square errors (RMSEs) of position and orientation are used as performance metrics, which are defined as

$$\begin{cases} \text{RMSE}_p^i(k) \\ = \sqrt{\frac{1}{M_n} \sum_{s=1}^{M_n} \left[\left(x_k^{i(s)} - \hat{x}_{k|k}^{i(s)} \right)^2 + \left(y_k^{i(s)} - \hat{y}_{k|k}^{i(s)} \right)^2 \right]} \\ \text{RMSE}_o^i(k) = \sqrt{\frac{1}{M_n} \sum_{s=1}^{M_n} \left(\phi_k^{i(s)} - \hat{\phi}_{k|k}^{i(s)} \right)^2} \end{cases} \quad (34)$$

where RMSE_p^i and RMSE_o^i denote the RMSEs of position and orientation of robot i , respectively, and $x_k^{i(s)}$, $y_k^{i(s)}$ and $\phi_k^{i(s)}$ are, respectively, the true values of east position, north position and orientation of robot i at the s th Monte Carlo simulation, and $\hat{x}_{k|k}^{i(s)}$, $\hat{y}_{k|k}^{i(s)}$ and $\hat{\phi}_{k|k}^{i(s)}$ are, respectively, the estimates of east position, north position and orientation of robot i at the s th Monte Carlo simulation, and M_n denotes the total numbers of Monte Carlo simulations.

To compare the estimation consistency, the normalized estimation error squared (NEES) is selected as the evaluation index, which is defined as follows:

$$\text{NEES}^i(k) = \frac{1}{M_n} \sum_{s=1}^{M_n} \left(\mathbf{x}_k^{i(s)} - \hat{\mathbf{x}}_{k|k}^{i(s)} \right)^T \left(\boldsymbol{\Sigma}_{k|k}^{i(s)} \right)^{-1} \left(\mathbf{x}_k^{i(s)} - \hat{\mathbf{x}}_{k|k}^{i(s)} \right) \quad (35)$$

TABLE VII

ARMSEs OF POSITION AND ORIENTATION, ANEESs, AND SINGLE STEP RUN TIMES OF ALL THE ALGORITHMS COMPARED FOR SIX MOBILE ROBOTS

CL Methods	Metrics	Robot 1	Robot 2	Robot 3	Robot 4	Robot 5	Robot 6
CCL-EKF	ARMSE _p (m)	0.09	0.11	0.12	0.09	0.10	0.09
	ARMSE _o (deg)	1.34	1.42	1.43	1.29	1.30	1.31
	ANEES	3.00	3.00	3.04	2.98	3.00	2.99
	Time (ms)	0.26	0.26	0.26	0.26	0.26	0.26
RDCL-EKF-T	ARMSE _p (m)	0.10	0.11	0.12	0.09	0.10	0.09
	ARMSE _o (deg)	1.34	1.42	1.43	1.29	1.30	1.32
	ANEES	3.54	3.48	3.44	3.50	3.20	3.47
	Time (ms)	0.10	0.10	0.10	0.10	0.10	0.10
RDCL-EKF-N	ARMSE _p (m)	0.22	0.27	0.29	0.20	0.25	0.21
	ARMSE _o (deg)	1.82	1.86	1.87	1.79	1.83	1.81
	ANEES	10.79	13.80	15.85	10.07	12.53	9.89
	Time (ms)	0.10	0.10	0.10	0.10	0.10	0.10
RDCL-EKF-VB	ARMSE _p (m)	0.12	0.13	0.14	0.11	0.13	0.11
	ARMSE _o (deg)	1.51	1.57	1.59	1.48	1.52	1.50
	ANEES	3.23	3.37	3.54	3.34	3.35	3.27
	Time (ms)	0.28	0.28	0.28	0.28	0.28	0.28

where NEES^{*i*} denotes the NEES of robot *i*, and $\mathbf{x}_k^{i(s)}$ is the true state vector of robot *i* at the *s*th Monte Carlo simulation, and $\hat{\mathbf{x}}_{k|k}^{i(s)}$ and $\Sigma_{k|k}^{i(s)}$ are, respectively, the state estimate and estimation error covariance matrix of robot *i* at the *s*th Monte Carlo simulation. In theory, if the state estimate is consistent, then the NEES value is not greater than the state dimension (i.e., NEES ≤ 3), and the state estimate is strictly consistent when the NEES value is identical to state dimension (i.e., NEES = 3).

To compare the estimation accuracy of absolute and relative measurement noise covariance matrices, the RMSEs of standard deviations of range and bearing measurements are used as evaluation metrics, which are defined as where RMSE_{σ_r} and RMSE_{σ_θ} denote, respectively, the RMSEs of standard deviations of range and bearing measurements, and $l_k^{i*(s)}$ and $j_k^{i*(s)}$ denote, respectively, the detected landmark and robot sets by robot *i* at time *k* of the *s*th Monte Carlo simulation, and $|l_k^{i*(s)}|$ denotes the number of landmarks within the set $l_k^{i*(s)}$, and $|j_k^{i*(s)}|$ denotes the number of mobile robots within the set

$j_k^{i*(s)}$, and $\hat{\sigma}_{r,ak|k}^{il(s)}$ and $\hat{\sigma}_{\theta,ak|k}^{il(s)}$ denote the estimates of standard deviations of absolute range and bearing measurements at time *k* of the *s*th Monte Carlo simulation, respectively, and $\hat{\sigma}_{r,rk|k}^{ij(s)}$ and $\hat{\sigma}_{\theta,rk|k}^{ij(s)}$ denote the estimates of standard deviations of relative range and bearing measurements at time *k* of the *s*th Monte Carlo simulation, respectively.

B. Simulation Results and Analyses

Figs. 9–11 show the RMSEs of position and orientation and the NEESs of all the algorithms compared for six mobile robots, respectively, and Table VII lists the averaged RMSEs (ARMSEs) of position and orientation, the averaged NEESs (ANEESs), and the single step run times of all the algorithms compared for six mobile robots, respectively. It is seen from Figs. 9 and 10 and Table VII that the proposed RDCL-EKF-VB method has similar RMSEs and ARMSEs of position and orientation to the RDCL-EKF-T but smaller RMSEs and ARMSEs of position and orientation than

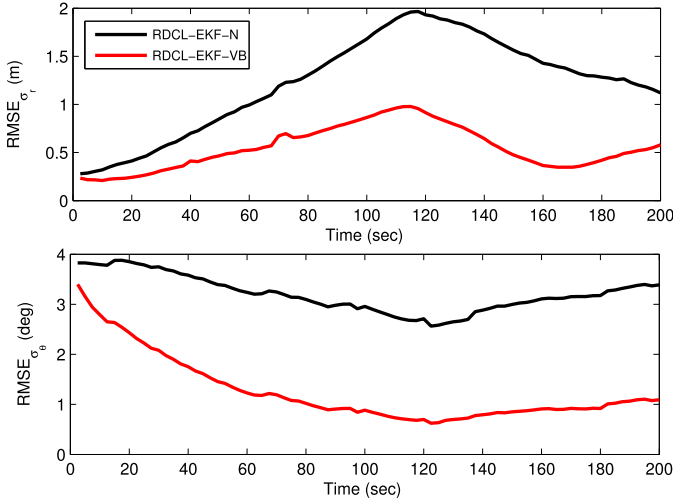
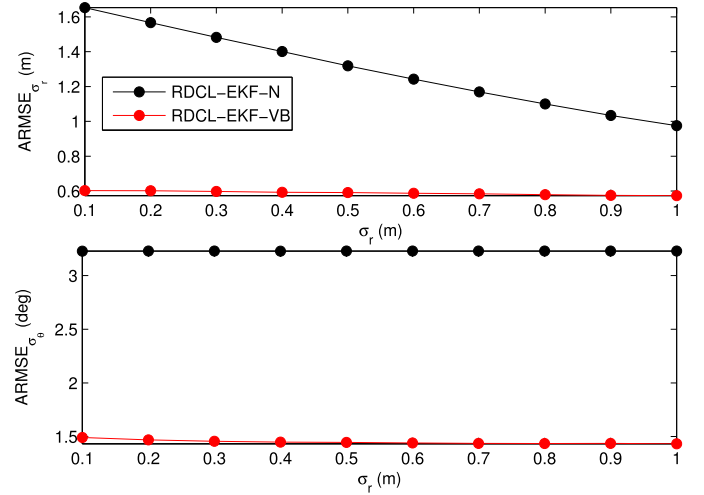
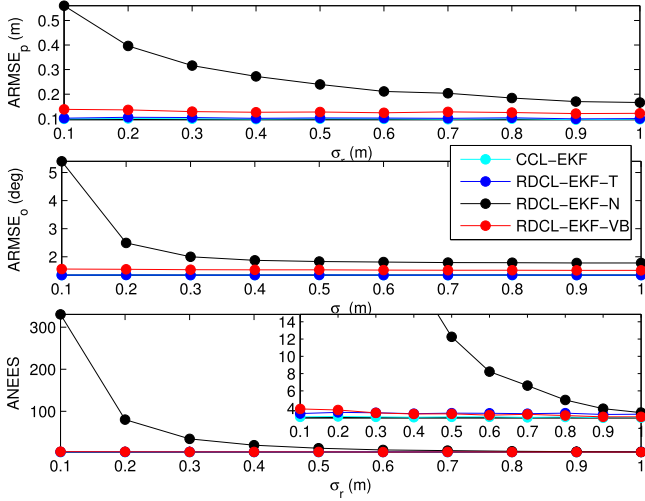
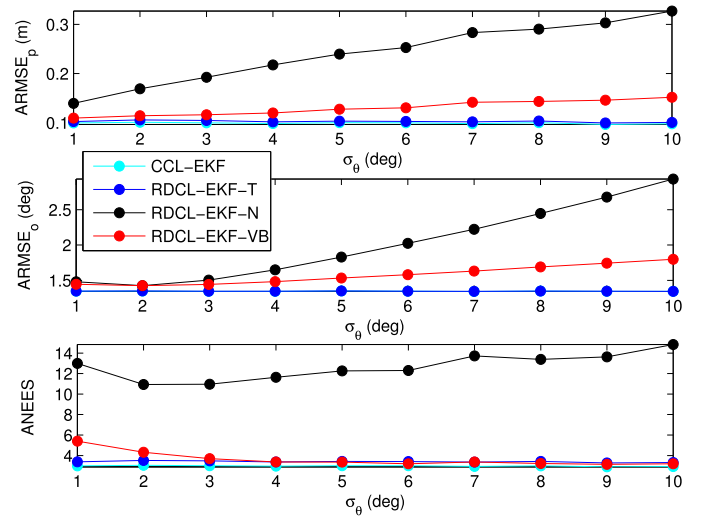


Fig. 12. RMSEs of standard deviations of range and bearing measurements.


 Fig. 14. ARMSEs of standard deviations of range and bearing measurements when $\bar{\sigma}_\theta = 5$ (deg) and $\bar{\sigma}_r = 0.1:0.1:1.0$ (m).

 Fig. 13. ARMSEs of position and orientation and ANEESs when $\bar{\sigma}_\theta = 5$ (deg) and $\bar{\sigma}_r = 0.1:0.1:1.0$ (m).

 Fig. 15. ARMSEs of position and orientation and ANEESs when $\bar{\sigma}_r = 0.5$ (m) and $\bar{\sigma}_\theta = 1:1:10$ (deg).

the existing RDCL-EKF-N method. It can be seen from Fig. 11 and Table VII that the NEESs and ANEESs of the proposed method and the RDCL-EKF-T are almost identical and all close to the benchmark 3, however, the NEESs and ANEESs of the existing RDCL-EKF-N method are all far from the benchmark 3. We can also see from Table VII that the proposed RDCL-EKF-VB method requires more single step run times than the existing RDCL-EKF-N method. Thus, the proposed RDCL-EKF-VB method has similar CL

accuracy and estimation consistency as the RDCL-EKF-T method but better CL accuracy and estimation consistency than the existing RDCL-EKF-N method at the cost of the increased computational complexity.

Fig. 12 illustrates the RMSEs of standard deviations of range and bearing measurements. We can see from Fig. 12 that the proposed RDCL-EKF-VB method has smaller $RMSE_{\sigma_r}$ and $RMSE_{\sigma_\theta}$ than the existing RDCL-EKF-N method. The

$$\left\{ \begin{array}{l} RMSE_{\sigma_r} = \sqrt{\frac{1}{M_n} \sum_{s=1}^{M_n} \sum_{i=1}^{n_R} \left[\frac{\sum_{l \in I_k^{i*(s)}} (\sigma_r - \hat{\sigma}_{r,ak|k}^{il(s)})^2}{\sum_{i=1}^{n_R} |I_k^{i*(s)}|} + \frac{\sum_{j \in J_k^{i*(s)}} (\sigma_r - \hat{\sigma}_{r,rk|k}^{ij(s)})^2}{\sum_{i=1}^{n_R} |J_k^{i*(s)}|} \right]} \\ RMSE_{\sigma_\theta} = \sqrt{\frac{1}{M_n} \sum_{s=1}^{M_n} \sum_{i=1}^{n_R} \left[\frac{\sum_{l \in I_k^{i*(s)}} (\sigma_\theta - \hat{\sigma}_{\theta,ak|k}^{il(s)})^2}{\sum_{i=1}^{n_R} |I_k^{i*(s)}|} + \frac{\sum_{j \in J_k^{i*(s)}} (\sigma_\theta - \hat{\sigma}_{\theta,rk|k}^{ij(s)})^2}{\sum_{i=1}^{n_R} |J_k^{i*(s)}|} \right]} \end{array} \right. \quad (36)$$

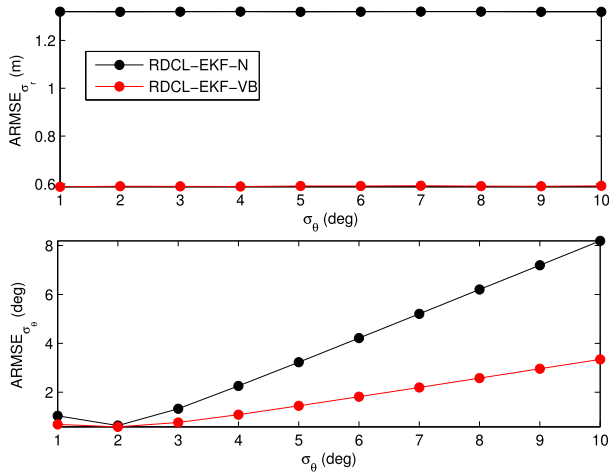


Fig. 16. ARMSEs of standard deviations of range and bearing measurements when $\bar{\sigma}_r = 0.5$ (m) and $\bar{\sigma}_\theta = 1:1:10$ (deg).

$ARMSE_{\sigma_r}$ and $ARMSE_{\sigma_\theta}$ of the existing RDCL-EKF-N method and the proposed RDCL-EKF-VB method are, respectively, 1.22 (m), 3.21 (deg), 0.54 (m), and 1.27 (deg). Thus, the proposed RDCL-EKF-VB method can better estimate the absolute and relative measurement noise covariance matrices than the existing RDCL-EKF-N method, which results in better CL accuracy and estimation consistency.

To better show the advantages of the proposed RDCL-EKF-VB method, the performances of all methods are further compared when different nominal standard deviations of range and bearing measurements are selected. Figs. 13 and 14 show the ARMSEs of position and orientation, ANEESs, and the ARMSEs of standard deviations of range and bearing measurements, respectively, when the nominal standard deviation of bearing measurement is chosen as $\bar{\sigma}_\theta = 5$ (deg) and the nominal standard deviation of range measurement is set as $\bar{\sigma}_r = 0.1 : 0.1 : 1.0$ (m). Figs. 15 and 16 give the ARMSEs of position and orientation, ANEESs, and the ARMSEs of standard deviations of range and bearing measurements, respectively, when the nominal standard deviation of range measurement is chosen as $\bar{\sigma}_r = 0.5$ (m) and the nominal standard deviation of bearing measurement is set as $\bar{\sigma}_\theta = 1 : 1 : 10$ (deg). It is observed from Figs. 13 and 15 that the proposed RDCL-EKF-VB method always has better CL accuracy and estimation consistency than the existing RDCL-EKF-N method when different standard deviations of range and bearing measurements are selected. It can be also observed from Figs. 14 and 16 that the proposed RDCL-EKF-VB method can always estimate the absolute and relative measurement noise covariance matrices better than the existing RDCL-EKF-N method when different standard deviations of range and bearing measurements are selected. Consequently, for the case of time-varying measurement accuracy, the CL accuracy and estimation consistency of the existing RDCL-EKF method can be further improved by the proposed method, which is induced by the recursively adaptive learning of the absolute and relative measurement noise covariance matrices based on online pose estimates and measurement data using the VB approach.



Fig. 17. Experimental field for UTIAS multirobot cooperative localization and mapping data set [42].

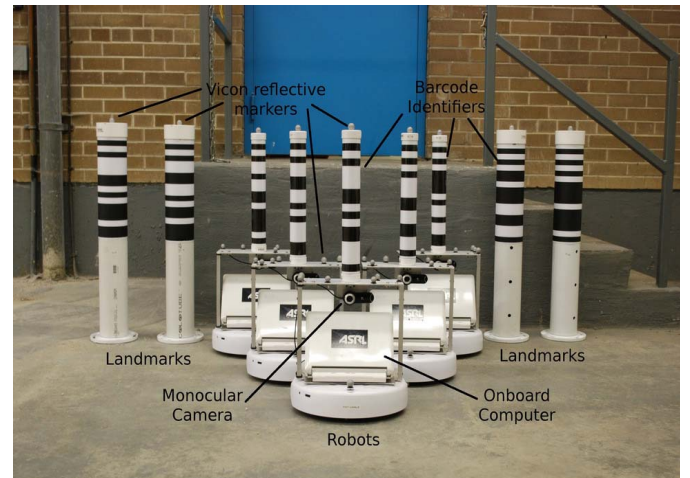


Fig. 18. Experimental platforms for UTIAS multirobot cooperative localization and mapping data set [42].

V. EXPERIMENT STUDY

A. Experimental Setups and Descriptions

In this section, the performance of the proposed adaptive RDCL-EKF algorithm is tested with an open access *UTIAS multirobot cooperative localization and mapping data set* that was provided by Leung *et al.* [42]. In the experiment, a team of five identical mobile robots moved on a flat lab with 15 landmarks, where the 15 cylindrical tubes with distinguishable barcode identifiers served as landmarks. Each robot was equipped with a wheel encoder and a monocular camera, in which the wheel encoder was used to measure the linear and rotational velocities of each robot with output frequency 67 (Hz), and the monocular camera was employed to obtain the range and bearing measurements between the robot and the landmark or the other robot. The reference positions of landmarks and the reference poses of all mobile robots were all provided by a 10-camera Vicon motion capture system at 100 (Hz) whose position accuracy is on the order of 1 (mm). The experimental field and platforms are, respectively, shown in Figs. 17 and 18.

TABLE VIII
APES, AOE, ANEES, AND SINGLE STEP RUN TIMES OF ALL THE ALGORITHMS COMPARED FOR FIVE MOBILE ROBOTS USING THE DATA 1

CL Methods	Metrics	Robot 1	Robot 2	Robot 3	Robot 4	Robot 5
CCL-EKF-N	APE (m)	0.10	0.09	0.08	0.10	0.10
	AOE (deg)	3.25	2.31	2.06	3.54	2.55
	ANEES	12.15	12.03	12.50	9.72	13.72
	Time (ms)	0.008	0.008	0.008	0.008	0.008
RDCL-EKF-N	APE (m)	0.35	0.40	0.25	0.56	0.31
	AOE (deg)	6.73	8.13	5.31	13.83	6.99
	ANEES	222.7	490.4	118.0	1462.5	214.0
	Time (ms)	0.008	0.008	0.008	0.008	0.008
RDCL-EKF-VB	APE (m)	0.15	0.14	0.11	0.23	0.13
	AOE (deg)	4.42	4.16	3.27	6.80	3.85
	ANEES	23.01	27.71	21.80	37.07	22.44
	Time (ms)	0.014	0.014	0.014	0.014	0.014

The motion model of each robot is described by (1), and the discretization time of the motion model is set as $\Delta t = 0.02$ (s). The range and bearing measurements between the robot and the landmark are described by the absolute measurement models in (2), and the range and bearing measurements between the robot and the other robot are modeled by the relative measurement models in (4). Eight sets of real-world data (i.e., data 1 to data 8) are used in this experiment study, which are, respectively, collected in eight different runs with different test trajectories, moving velocities, and running times ranging from 15 to 70 (min). To demonstrate the effectiveness and superiority of the proposed method, three CL-EKF algorithms are compared in the experimental tests, including CCL-EKF-N, RDCL-EKF-N, and RDCL-EKF-VB, where CCL-EKF-N is the existing CCL-EKF algorithm using the nominal absolute and relative measurement noise covariance matrices \mathbf{R}_{ak} and \mathbf{R}_{rk} to estimate the poses of all robots as reference, and the descriptions and parameter settings of the RDCL-EKF-N and RDCL-EKF-VB in the experiment study are the same as those in the simulation study. Note that the CCL-EKF-N algorithm is used as an optimal benchmark for CL. Since the true state and measurement noise covariance matrices are unknown in the test, their nominal values are used in the CCL-EKF-N, RDCL-EKF-N, and RDCL-EKF-VB. In the experimental comparisons, the nominal state noise covariance matrix is selected as $\mathbf{Q}_k = \text{diag}\{\{\bar{\sigma}_v^2, \bar{\sigma}_\Omega^2\}\}$, where $\bar{\sigma}_v = (\sqrt{2}/2)\bar{\sigma}$ and $\bar{\sigma}_\Omega = (2\sqrt{2}/\bar{\sigma})$ with $\bar{\sigma} = 0.1$, and the nominal absolute and

relative measurement noise covariance matrices are chosen as $\mathbf{R}_{ak} = \mathbf{R}_{rk} = \text{diag}\{\{\bar{\sigma}_r^2, \bar{\sigma}_\theta^2\}\}$ with nominal standard deviations $\bar{\sigma}_r = 0.5$ (m) and $\bar{\sigma}_\theta = 3$ (deg). The codes of all algorithms are performed on a computer with Intel Core i7-6500U CPU at 2.50 GHz.

To compare the CL accuracy, the position error (PE) and the orientation error (OE) are selected as performance metrics, which are defined as follows:

$$\begin{cases} \text{PE}^i(k) = \sqrt{(x_{rk}^i - \hat{x}_{k|k}^i)^2 + (y_{rk}^i - \hat{y}_{k|k}^i)^2} \\ \text{OE}^i(k) = |\phi_{rk}^i - \hat{\phi}_{k|k}^i| \end{cases} \quad (37)$$

where PE^i and OE^i denote the PE and OE of robot i , respectively, and x_{rk}^i , y_{rk}^i , and ϕ_{rk}^i are, respectively, the reference values of east position, north position, and orientation of robot i , and $\hat{x}_{k|k}^i$, $\hat{y}_{k|k}^i$, and $\hat{\phi}_{k|k}^i$ are, respectively, the estimates of east position, north position, and orientation of robot i . Like as in the simulation study, the NEES is used to evaluate the estimation consistency, but M_n is set as 1 in the experiment study. To better show the results of experimental comparisons, the PEs, OEs, and NEESs of all the algorithms compared are smoothed with a span of 20 (s).

B. Experimental Results and Analyses

First, we compare the PEs, OEs, and NEESs of the CCL-EKF-N, RDCL-EKF-N, and RDCL-EKF-VB using the data 1.

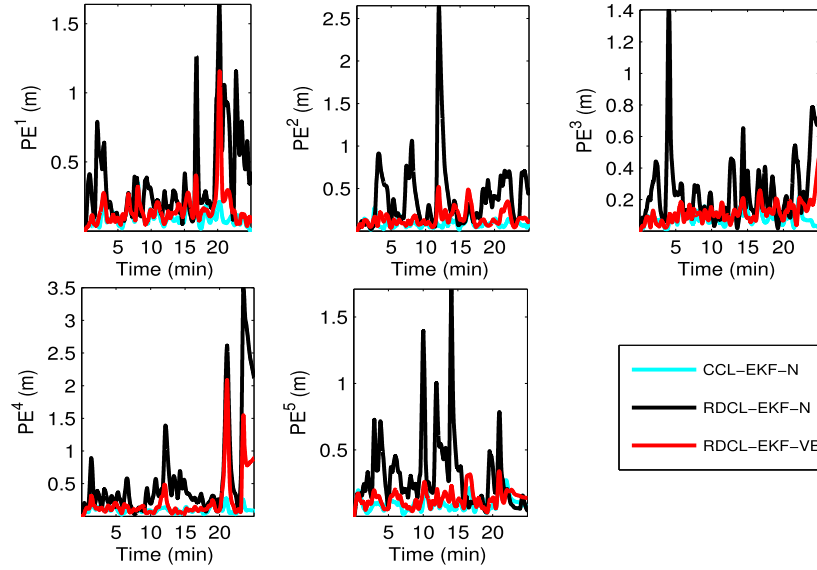


Fig. 19. PEs of all the algorithms compared for five mobile robots using the data 1.

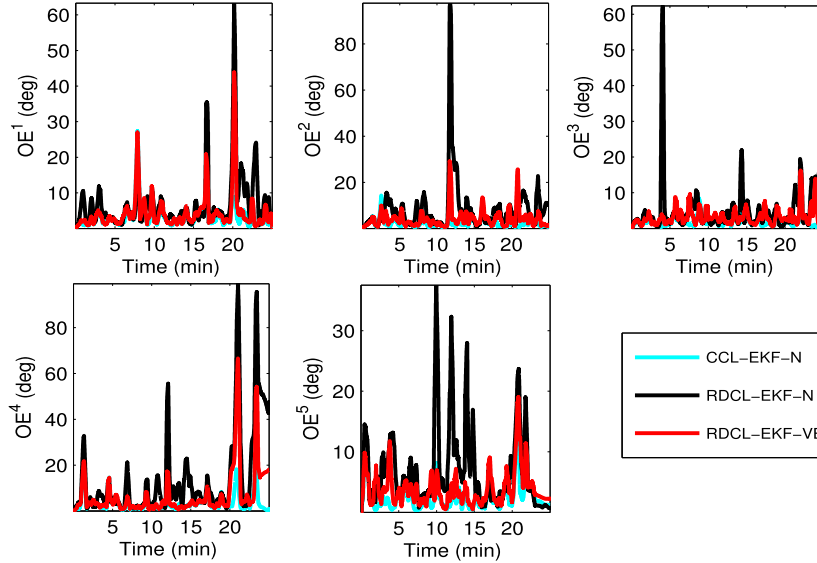


Fig. 20. OEs of all the algorithms compared for five mobile robots using the data 1.

It is noted that the similar results can be also obtained using data 2 to data 8, so they are omitted for brevity. The PEs, OEs, and NEESs of all the algorithms compared for five mobile robots are, respectively, shown in Figs. 19–21. The averaged PEs (APEs), averaged OEs (AOEs), ANEESs, and single step run times of all the algorithms compared for five mobile robots are given in Table VIII. It can be seen from Figs. 19 and 20 and Table VIII that the proposed RDCL-EKF-VB algorithm has smaller PEs, OEs, APEs, and AOE than the existing RDCL-EKF-N algorithm. We can also see from Fig. 21 and Table VIII that the NEESs and ANEESs of the proposed RDCL-EKF-VB algorithm are closer to 3 as compared with those of the existing RDCL-EKF-N algorithm. Meanwhile, as shown in Table VIII, the proposed RDCL-EKF-VB algorithm has greater single step run times than the existing RDCL-EKF-N algorithm. It can be seen that the proposed RDCL-EKF-VB algorithm

has better CL accuracy and estimation consistency but slightly greater implementation load than the existing RDCL-EKF-N algorithm for the real-world data 1, which results from the use of the more accurate measurement noise covariance matrices.

Second, we aim to test the dependence of the proposed method on the selections of nominal standard deviations of range and bearing measurements. To this end, the overall APEs (OAPEs), overall AOE (OAOEs) and overall ANEESs (OANEESs) among all robots are used to compare the performance, which are defined as

$$\begin{aligned} \text{OAPE} &= \frac{1}{n_R} \sum_{i=1}^{n_R} \text{APE}^i, & \text{OAOE} &= \frac{1}{n_R} \sum_{i=1}^{n_R} \text{AOE}^i, \\ \text{OANEES} &= \frac{1}{n_R} \sum_{i=1}^{n_R} \text{ANEES}^i \end{aligned} \quad (38)$$

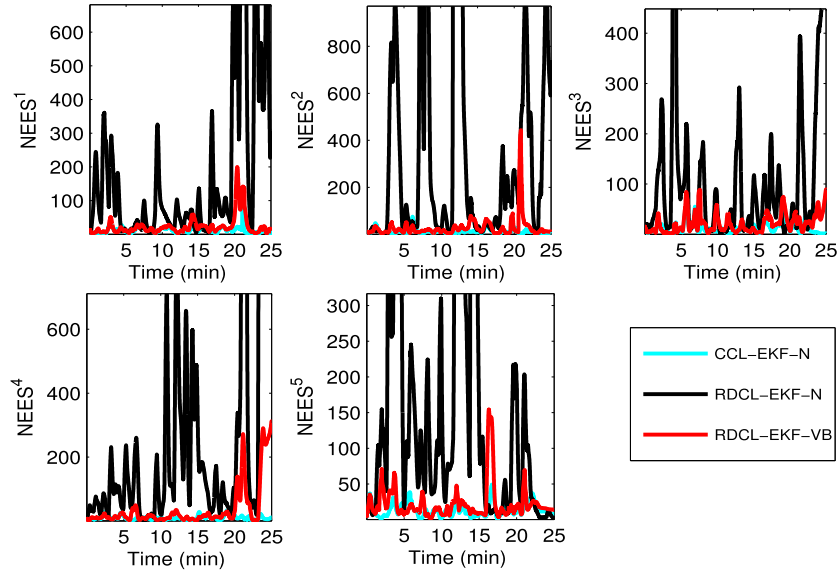


Fig. 21. NEESs of all the algorithms compared for five mobile robots using the data 1.

TABLE IX
OAPES, OAOES, AND OANEESs OF ALL THE ALGORITHMS COMPARED USING DATA 1–8

CL Methods	Metrics	Data 1	Data 2	Data 3	Data 4	Data 5	Data 6	Data 7	Data 8
CCL-EKF-N	APE (m)	0.09	0.10	0.08	0.08	0.11	0.09	0.12	0.11
	AOE (deg)	2.74	3.04	2.46	2.21	3.89	3.30	3.18	4.65
	ANEES	12.03	14.55	11.87	13.65	9.98	9.80	18.59	14.04
RDCL-EKF-N	APE (m)	0.37	0.41	0.31	0.32	0.98	0.35	0.38	0.47
	AOE (deg)	8.20	9.07	6.67	6.25	24.77	8.89	8.12	13.39
	ANEES	501.5	365.8	233.2	286.7	1108.1	233.1	247.3	535.35
RDCL-EKF-VB	APE (m)	0.15	0.17	0.14	0.12	0.39	0.18	0.19	0.24
	AOE (deg)	4.50	5.15	4.02	3.49	9.89	5.29	4.92	8.53
	ANEES	26.41	32.40	27.95	27.31	75.48	73.05	47.68	42.02

where APE^i , AOE^i , and $ANEES^i$ denote, respectively, the APE, AOE, and ANEES of robot i , and OAPE, OAOE, and OANEES denote, respectively, the overall APE, AOE, and ANEES among all robots.

We compare the OAPES, OAOES, and OANEESs of the CCL-EKF-N, RDCL-EKF-N, and RDCL-EKF-VB using the data 1 when different nominal standard deviations of range and bearing measurements are selected. Fig. 22 illustrates the OAPES, OAOES, and OANEESs of the CCL-EKF-N, RDCL-EKF-N, and RDCL-EKF-VB when the nominal standard deviation of bearing measurement is chosen as $\bar{\sigma}_\theta = 5$ (deg) and the nominal standard deviation of range measurement is set

as $\bar{\sigma}_r = 0.1 : 0.1 : 1.0$ (m). Fig. 23 exhibits the OAPES, OAOES, and OANEESs of the CCL-EKF-N, RDCL-EKF-N, and RDCL-EKF-VB when the nominal standard deviation of range measurement is chosen as $\bar{\sigma}_r = 0.5$ (m) and the nominal standard deviation of bearing measurement is set as $\bar{\sigma}_\theta = 1 : 1 : 10$ (deg). It can be observed from Figs. 22 and 23 that the proposed RDCL-EKF-VB algorithm always has better CL accuracy and estimation consistency than the existing RDCL-EKF-N algorithm when $\bar{\sigma}_r = 0.1 : 0.1 : 1.0$ (m) and $\bar{\sigma}_\theta = 1 : 1 : 10$ (deg), which exhibits the weak dependence of the proposed method on the selections of nominal standard deviations of range and bearing measurements. The underlying

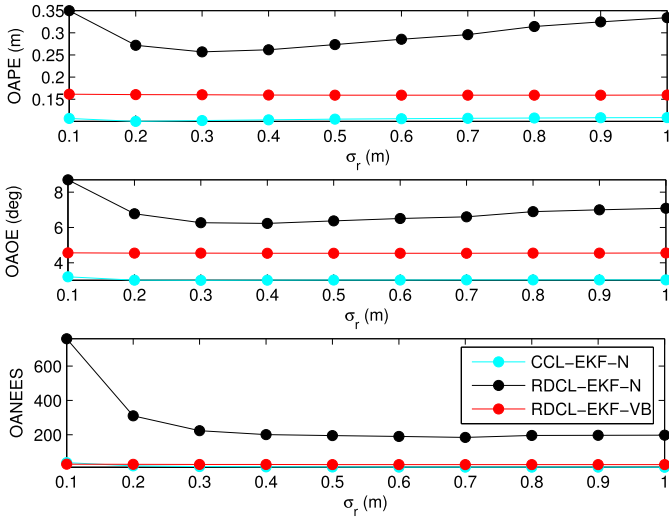


Fig. 22. OAPEs, OAOEs, and OANEESs when $\bar{\sigma}_\theta = 5$ (deg) and $\bar{\sigma}_r = 0.1:1.0$ (m) using the data 1.

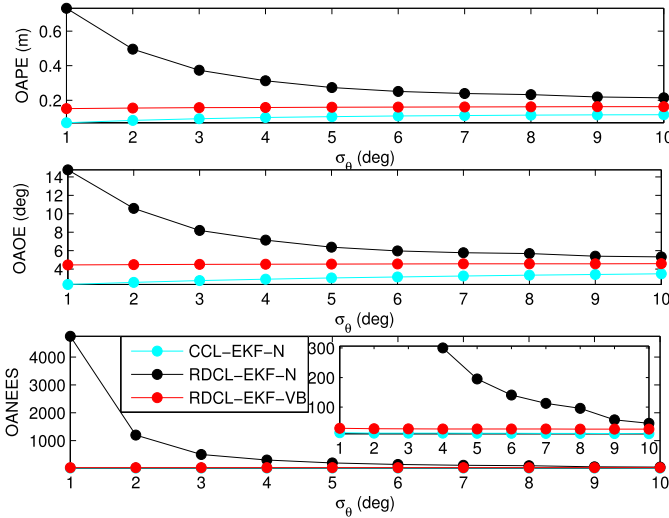


Fig. 23. OAPEs, OAOEs, and OANEESs when $\bar{\sigma}_r = 0.5$ (m) and $\bar{\sigma}_\theta = 1:10$ (deg) using the data 1.

cause is that the dependence on the nominal values of the measurement noise covariance matrices will decrease as the number of time updates for them increases.

To better exhibit the practicability of the proposed method, we compare the OAPEs, OAOEs, and OANEESs of the CCL-EKF-N, RDCL-EKF-N, and RDCL-EKF-VB using data 1–8. Table IX lists the OAPEs, OAOEs, and OANEESs of all the algorithms compared using data 1–8. We can observe from Table IX that the proposed RDCL-EKF-VB algorithm always has better CL accuracy and estimation consistency than the existing RDCL-EKF-N algorithm for data 1–8, which demonstrates the superiority of the proposed method in practical CL application.

VI. CONCLUSION

In this article, a novel adaptive RDCL-EKF method was proposed for multirobot systems with time-varying

measurement accuracy, where a novel decentralized estimation strategy was proposed for estimating the unknown absolute and relative measurement noise covariance matrices in a decentralized manner. For each robot, its pose and absolute and relative measurement noise covariance matrices were jointly inferred based on the constructed hierarchical Gaussian model using the VB approach. The proposed adaptive RDCL-EKF method has the same mode and number of communications as the standard RDCL-EKF method, but only requires slightly higher communication capacities to transmit additional parameters in each cooperation. A large number of simulations and real-world data sets were used to compare the proposed adaptive RDCL-EKF method and the existing RDCL-EKF method. Simulation and experimental results have demonstrated that the proposed adaptive RDCL-EKF method has better CL accuracy and estimation consistency but slightly heavier computational burden than the existing RDCL-EKF method for multirobot systems with time-varying measurement accuracy.

APPENDIX

A. Proofs of Propositions 1 and 2

Before solving $q^{(a)}(\mathbf{x}_k^i)$ and $q^{(a)}(\mathbf{R}_{ak}^{il})$, the joint PDF $p(\mathbf{x}_k^i, \{\hat{\mathbf{R}}_{ak}^{il}\}_{l \in I_k^{i*}}, \mathbf{z}_{1:k-1}, \{\mathbf{z}_{ak}^{il}\}_{l \in I_k^{i*}})$ in (14) and (15) is first calculated. According to Bayes' theorem and using (6)–(8) yields

$$\begin{aligned} & p(\mathbf{x}_k^i, \{\hat{\mathbf{R}}_{ak}^{il}\}_{l \in I_k^{i*}}, \mathbf{z}_{1:k-1}, \{\mathbf{z}_{ak}^{il}\}_{l \in I_k^{i*}}) \\ &= p(\mathbf{z}_{1:k-1}) p(\mathbf{x}_k^i | \mathbf{z}_{1:k-1}) \prod_{l \in I_k^{i*}} p(\mathbf{z}_{ak}^{il} | \mathbf{x}_k^i, \mathbf{R}_{ak}^{il}) \\ & \quad \times p(\mathbf{R}_{ak}^{il} | \mathbf{z}_{1:k-1}) = p(\mathbf{z}_{1:k-1}) \mathcal{N}(\mathbf{x}_k^i; \hat{\mathbf{x}}_{k|k-1}^i, \boldsymbol{\Sigma}_{k|k-1}^i) \\ & \quad \times \prod_{l \in I_k^{i*}} \mathcal{N}(\mathbf{z}_{ak}^{il}; \mathbf{h}_{ak}^{il}(\mathbf{x}_k^i, \mathbf{x}_L^l), \mathbf{R}_{ak}^{il}) \times \text{IW}(\mathbf{R}_{ak}^{il}; u_{ak|k-1}^{il}, \mathbf{U}_{ak|k-1}^{il}). \end{aligned} \quad (39)$$

Next, we solve $q^{(a)}(\mathbf{x}_k^i)$ and $q^{(a)}(\mathbf{R}_{ak}^{il})$. Substituting (39) in (14), we have

$$\begin{aligned} \log q^{(a)}(\mathbf{x}_k^i) &= \log \mathcal{N}(\mathbf{x}_k^i; \hat{\mathbf{x}}_{k|k-1}^i, \boldsymbol{\Sigma}_{k|k-1}^i) \\ & \quad + \sum_{l \in I_k^{i*}} \log \mathcal{N}(\mathbf{z}_{ak}^{il}; \mathbf{h}_{ak}^{il}(\mathbf{x}_k^i, \mathbf{x}_L^l), \hat{\mathbf{R}}_{ak}^{il}) + c_{\mathbf{x}_k^i}. \end{aligned} \quad (40)$$

By linearizing the absolute measurement functions $\{\mathbf{h}_{ak}^{il}(\mathbf{x}_k^i, \mathbf{x}_L^l)\}_{l \in I_k^{i*}}$ at $\mathbf{x}_k^i = \hat{\mathbf{x}}_{k|k-1}^i$ and exploiting (40), $q^{(a)}(\mathbf{x}_k^i)$ can be approximately updated as (16).

Substituting (39) in (15) gives

$$\begin{aligned} \log q^{(a)}(\mathbf{R}_{ak}^{il}) &= -\frac{1}{2} (n_a + u_{ak|k-1}^{il} + 2) \log |\mathbf{R}_{ak}^{il}| \\ & \quad - \frac{1}{2} \text{tr} \left\{ (\mathbf{U}_{ak|k-1}^{il} + \mathbf{A}_k^{il}) (\mathbf{R}_{ak}^{il})^{-1} \right\} + c_{\mathbf{R}_{ak}^{il}} \end{aligned} \quad (41)$$

where $\text{tr}(\cdot)$ denotes the trace operation of a matrix.

According to the definition of the inverse-Wishart PDF, $q^{(a)}(\mathbf{R}_{ak}^{il})$ can be updated as (18).

B. Proofs of Propositions 3 and 4

First, we calculate the joint PDF in (24) and (25) as follows. According to the conditional independence and Bayes' theorem, the joint PDF can be factored as

$$\begin{aligned} & p\left(\mathbf{x}_k^i, \{\mathbf{x}_k^j\}_{j \in j_k^{i*}}, \{\mathbf{R}_{rk}^{ij}\}_{j \in j_k^{i*}}, \mathbf{z}_{1:k-1}, \{\mathbf{z}_{ak}^{il}\}_{l \in l_k^{i*}}, \{\mathbf{z}_{rk}^{ij}\}_{j \in j_k^{i*}}\right) \\ &= p\left(\mathbf{z}_{1:k-1}, \{\mathbf{z}_{ak}^{il}\}_{l \in l_k^{i*}}\right) \\ & \quad \times p\left(\mathbf{x}_k^i, \{\mathbf{x}_k^j\}_{j \in j_k^{i*}} \middle| \mathbf{z}_{1:k-1}, \{\mathbf{z}_{ak}^{il}\}_{l \in l_k^{i*}}\right) \\ & \quad \times \prod_{j \in j_k^{i*}} p\left(\mathbf{z}_{rk}^{ij} | \mathbf{x}_k^i, \mathbf{x}_k^j, \mathbf{R}_{rk}^{ij}\right) p\left(\mathbf{R}_{rk}^{ij} | \mathbf{z}_{1:k-1}, \{\mathbf{z}_{ak}^{il}\}_{l \in l_k^{i*}}\right). \end{aligned} \quad (42)$$

Exploiting the variational approximation to $p(\mathbf{x}_k^i | \mathbf{z}_{1:k-1}, \{\mathbf{z}_{ak}^{il}\}_{l \in l_k^{i*}})$ in (13) and (16), the joint posterior PDF $p(\mathbf{x}_k^i, \{\mathbf{x}_k^j\}_{j \in j_k^{i*}} | \mathbf{z}_{1:k-1}, \{\mathbf{z}_{ak}^{il}\}_{l \in l_k^{i*}})$ can be approximated as Gaussian, that is

$$\begin{aligned} & p\left(\mathbf{x}_k^i, \{\mathbf{x}_k^j\}_{j \in j_k^{i*}} \middle| \mathbf{z}_{1:k-1}, \{\mathbf{z}_{ak}^{il}\}_{l \in l_k^{i*}}\right) \\ &= \mathbf{N}\left(\begin{bmatrix} \mathbf{x}_k^i \\ \mathbf{x}_k^j \end{bmatrix}; \begin{bmatrix} \hat{\mathbf{x}}_{k|k}^{i(a)} \\ \hat{\mathbf{x}}_{k|k}^{j*} \end{bmatrix}, \begin{bmatrix} \Sigma_{k|k}^{i(a)} & \Sigma_{k|k}^{ij*} \\ \left(\Sigma_{k|k}^{ij*}\right)^T & \Sigma_{k|k}^{j*} \end{bmatrix}\right) \end{aligned} \quad (43)$$

where the augmented state vector is defined as $\mathbf{x}_k^{j*} \triangleq \text{col}\{\mathbf{x}_k^j\}_{j \in j_k^{i*}}$, and the state estimates $\hat{\mathbf{x}}_{k|k}^{i(a)}$ and $\hat{\mathbf{x}}_{k|k}^{j*}$, the error covariance matrices $\Sigma_{k|k}^{i(a)}$ and $\Sigma_{k|k}^{j*}$, and the cross correlation $\Sigma_{k|k}^{ij*}$ are all defined in Table III, which can be obtained by running the LAMU function with the estimated absolute measurement noise covariance matrices.

Using (10), (11), and (43) in (42), we have

$$\begin{aligned} & p\left(\mathbf{x}_k^i, \{\mathbf{x}_k^j\}_{j \in j_k^{i*}}, \{\mathbf{R}_{rk}^{ij}\}_{j \in j_k^{i*}}, \mathbf{z}_{1:k-1}, \{\mathbf{z}_{ak}^{il}\}_{l \in l_k^{i*}}, \{\mathbf{z}_{rk}^{ij}\}_{j \in j_k^{i*}}\right) \\ &= \mathbf{N}\left(\begin{bmatrix} \mathbf{x}_k^i \\ \mathbf{x}_k^j \end{bmatrix}; \begin{bmatrix} \hat{\mathbf{x}}_{k|k}^{i(a)} \\ \hat{\mathbf{x}}_{k|k}^{j*} \end{bmatrix}, \begin{bmatrix} \Sigma_{k|k}^{i(a)} & \Sigma_{k|k}^{ij*} \\ \left(\Sigma_{k|k}^{ij*}\right)^T & \Sigma_{k|k}^{j*} \end{bmatrix}\right) \\ & \quad \times p\left(\mathbf{z}_{1:k-1}, \{\mathbf{z}_{ak}^{il}\}_{l \in l_k^{i*}}\right) \times \\ & \quad \prod_{j \in j_k^{i*}} \mathbf{N}\left(\mathbf{z}_{rk}^{ij}; \mathbf{h}_{rk}^{ij}(\mathbf{x}_k^i, \mathbf{x}_k^j), \mathbf{R}_{rk}^{ij}\right) \text{IW}\left(\mathbf{R}_{rk}^{ij}; u_{rk|k-1}^{ij}, \mathbf{U}_{rk|k-1}^{ij}\right). \end{aligned} \quad (44)$$

Secondly, we calculate the approximate posterior PDFs $q(\mathbf{x}_k^i, \{\mathbf{x}_k^j\}_{j \in j_k^{i*}})$ and $q(\mathbf{R}_{rk}^{ij})$. Substituting (44) in (24) yields

$$\begin{aligned} & \log q\left(\mathbf{x}_k^i, \{\mathbf{x}_k^j\}_{j \in j_k^{i*}}\right) \\ &= \log \mathbf{N}\left(\begin{bmatrix} \mathbf{x}_k^i \\ \mathbf{x}_k^j \end{bmatrix}; \begin{bmatrix} \hat{\mathbf{x}}_{k|k}^{i(a)} \\ \hat{\mathbf{x}}_{k|k}^{j*} \end{bmatrix}, \begin{bmatrix} \Sigma_{k|k}^{i(a)} & \Sigma_{k|k}^{ij*} \\ \left(\Sigma_{k|k}^{ij*}\right)^T & \Sigma_{k|k}^{j*} \end{bmatrix}\right) \\ & \quad + \sum_{j \in j_k^{i*}} \log \mathbf{N}\left(\mathbf{z}_{rk}^{ij}; \mathbf{h}_{rk}^{ij}(\mathbf{x}_k^i, \mathbf{x}_k^j), \hat{\mathbf{R}}_{rk}^{ij}\right) + c\left\{\mathbf{x}_k^i, \{\mathbf{x}_k^j\}_{j \in j_k^{i*}}\right\}. \end{aligned} \quad (45)$$

By linearizing the relative measurement function $\mathbf{h}_{rk}^{ij}(\mathbf{x}_k^i, \mathbf{x}_k^j)$ at $\{\mathbf{x}_k^i = \hat{\mathbf{x}}_{k|k}^{i(a)}, \mathbf{x}_k^j = \hat{\mathbf{x}}_{k|k}^{j*}\}$ and exploiting (45), $q(\mathbf{x}_k^i, \{\mathbf{x}_k^j\}_{j \in j_k^{i*}})$ can be approximately updated as (26).

Substituting (44) in (25) gives

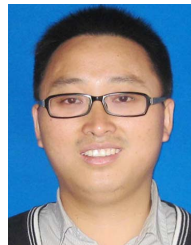
$$\begin{aligned} \log q\left(\mathbf{R}_{rk}^{ij}\right) &= -\frac{1}{2}\left(n_r + u_{rk|k-1}^{ij} + 2\right) \log \left|\mathbf{R}_{rk}^{ij}\right| \\ & \quad - \frac{1}{2} \text{tr}\left\{\left(\mathbf{U}_{rk|k-1}^{ij} + \mathbf{B}_k^{ij}\right)\left(\mathbf{R}_{rk}^{ij}\right)^{-1}\right\} + c_{\mathbf{R}_k^{ij}}. \end{aligned} \quad (46)$$

According to the definition of the inverse-Wishart distribution, the posterior PDF $q(\mathbf{R}_{rk}^{ij})$ is updated as (28).

REFERENCES

- [1] M. S. Miah and J. Knoll, "Area coverage optimization using heterogeneous robots: Algorithm and implementation," *IEEE Trans. Instrum. Meas.*, vol. 67, no. 6, pp. 1380–1388, Jun. 2018.
- [2] T. L. Huntsberger, A. Trebi-Ollennu, H. Aghazarian, P. S. Schenker, P. Pirjanian, and H. D. Nayar, "Distributed control of multi-robot systems engaged in tightly coupled tasks," *Auto. Robots*, vol. 17, no. 1, pp. 79–92, Jul. 2004.
- [3] A. D. Tews, G. S. Sukhatme, and M. J. Mataric, "A multi-robot approach to stealthy navigation in the presence of an observer," in *Proc. IEEE Int. Conf. Robot. Autom. (ICRA)*, vol. 1. New Orleans, LA, USA, Apr./May 2004, pp. 2379–2385.
- [4] Y. Feng, Z. Zhu, and J. Xiao, "Heterogeneous multi-robot localization in unknown 3D space," in *Proc. IEEE/RSJ Int. Conf. Intell. Robots Syst.*, Beijing, China, Oct. 2006, pp. 4533–4538.
- [5] R. G. Lins, S. N. Givigi, and P. G. Kurka, "Vision-based measurement for localization of objects in 3-D for robotic applications," *IEEE Trans. Instrum. Meas.*, vol. 64, no. 11, pp. 2950–2958, Nov. 2015.
- [6] H. Gietler, H. Ammari, and H. Zangl, "Robust electromagnetic pose estimation for robotic applications," *IEEE Trans. Instrum. Meas.*, vol. 69, no. 7, pp. 4258–4269, Jul. 2019.
- [7] P. Zhu and W. Ren, "Fully distributed joint localization and target tracking with mobile robot networks," *IEEE Trans. Control Syst. Technol.*, early access, Sep. 14, 2020, doi: 10.1109/TCST.2020.2991126.
- [8] S. I. Roumeliotis and G. A. Bekey, "Distributed multirobot localization," *IEEE Trans. Robot. Automat.*, vol. 18, no. 5, pp. 781–795, Oct. 2002.
- [9] Q. Li, Y. Ben, S. M. Naqvi, J. A. Neasham, and J. A. Chambers, "Robust Student's *t*-based cooperative navigation for autonomous underwater vehicles," *IEEE Trans. Instrum. Meas.*, vol. 67, no. 8, pp. 1762–1777, Aug. 2018.
- [10] S. S. Kia, S. F. Rounds, and S. Martinez, "A centralized-equivalent decentralized implementation of extended Kalman filters for cooperative localization," in *Proc. IEEE/RSJ Int. Conf. Intell. Robots Syst.*, Sep. 2014, pp. 3761–3766.
- [11] D. Fox, W. Burgard, H. Kruppa, and S. Thrun, "A probabilistic approach to collaborative multi-robot localization," *Auto. Robots*, vol. 8, no. 3, pp. 325–344, Jun. 2000.
- [12] A. Prorok, A. Bahr, and A. Martinoli, "Low-cost collaborative localization for large-scale multi-robot systems," in *Proc. IEEE Int. Conf. Robot. Automat. (ICRA)*, May 2012, pp. 4236–4241.
- [13] A. Howard, M. J. Mataric, and G. S. Sukhatme, "Localization for mobile robot teams using maximum likelihood estimation," in *Proc. IEEE/RSJ Int. Conf. Intell. Robots Syst. (IROS)*, Sep./Oct. 2002, pp. 434–439.
- [14] E. D. Nerurkar, S. I. Roumeliotis, and A. Martinelli, "Distributed maximum a posteriori estimation for multi-robot cooperative localization," in *Proc. IEEE Int. Conf. Robot. Autom.*, May 2009, pp. 1402–1409.
- [15] G. P. Huang, N. Trawny, A. I. Mourikis, and S. I. Roumeliotis, "Observability-based consistent EKF estimators for multi-robot cooperative localization," *Auto. Robots*, vol. 30, no. 1, pp. 99–122, Jan. 2011.
- [16] A. Martinelli and R. Siegwart, "Observability analysis for mobile robot localization," in *Proc. IEEE/RSJ Int. Conf. Intell. Robots Syst.*, Aug. 2005, pp. 1471–1476.

- [17] A. Martinelli, "Improving the precision on multi robot localization by using a series of filters hierarchically distributed," in *Proc. IEEE/RSJ Int. Conf. Intell. Robots Syst.*, Oct. 2007, pp. 1053–1058.
- [18] H. Mu, T. Bailey, P. Thompson, and H. Durrant-Whyte, "Decentralised solutions to the cooperative multi-platform navigation problem," *IEEE Trans. Aerosp. Electron. Syst.*, vol. 47, no. 2, pp. 1433–1449, Apr. 2011.
- [19] T. Bailey, M. Bryson, H. Mu, J. Vial, L. McCalman, and H. Durrant-Whyte, "Decentralised cooperative localisation for heterogeneous teams of mobile robots," in *Proc. IEEE Int. Conf. Robot. Automat. (ICRA)*, May 2011, pp. 2859–2865.
- [20] T. R. Wanasinghe, G. K. I. Mann, and R. G. Gosine, "Distributed leader-assistive localization method for a heterogeneous multirobotic system," *IEEE Trans. Autom. Sci. Eng.*, vol. 12, no. 3, pp. 795–809, Jul. 2015.
- [21] S. S. Kia, S. Rounds, and S. Martínez, "Cooperative localization for mobile agents: A recursive decentralized algorithm based on Kalman-filter decoupling," *IEEE Control Syst. Mag.*, vol. 36, no. 2, pp. 86–101, Apr. 2016.
- [22] H. Li and F. Nashashibi, "Cooperative multi-vehicle localization using split covariance intersection filter," in *Proc. IEEE Intell. Vehicles Symp.*, Alcalá de Henares, Spain, Jun. 2012, pp. 211–216.
- [23] L. C. Carrillo-Arce, E. D. Nerurkar, J. L. Gordillo, and S. I. Roumeliotis, "Decentralized multi-robot cooperative localization using covariance intersection," in *Proc. IEEE/RSJ Int. Conf. Intell. Robots Syst.*, Nov. 2013, pp. 1412–1417.
- [24] J. Zhu and S. S. Kia, "Cooperative localization under limited connectivity," *IEEE Trans. Robot.*, vol. 35, no. 6, pp. 1523–1530, Dec. 2019.
- [25] L. Luft, T. Schubert, S. I. Roumeliotis, and W. Burgard, "Recursive decentralized localization for multi-robot systems with asynchronous pairwise communication," *Int. J. Robot. Res.*, vol. 37, no. 10, pp. 1152–1167, Oct. 2018.
- [26] A. Bahr, M. R. Walter, and J. J. Leonard, "Consistent cooperative localization," in *Proc. IEEE Int. Conf. Robot. Automat. (ICRA)*, May 2009, pp. 3415–3422.
- [27] S. J. Julier and J. K. Uhlmann, "A non-divergent estimation algorithm in the presence of unknown correlations," in *Proc. Amer. Control Conf.*, Albuquerque, NM, USA, Jun. 1997, pp. 2369–2373.
- [28] S. J. Julier and J. K. Uhlmann, "General decentralized data fusion with covariance intersection (CI)," in *Handbook Data Fusion*. Boca Raton, FL, USA: CRC Press, 2001, pp. 272–276.
- [29] M. Ghobadi, P. Singla, and E. T. Esfahani, "Robust attitude estimation from uncertain observations of inertial sensors using covariance inflated multiplicative extended Kalman filter," *IEEE Trans. Instrum. Meas.*, vol. 67, no. 1, pp. 209–217, Jan. 2018.
- [30] A. H. Mohamed and K. P. Schwarz, "Adaptive Kalman filtering for INS/GPS," *J. Geodesy*, vol. 73, no. 4, pp. 193–203, May 1999.
- [31] F. Jiancheng and Y. Sheng, "Study on innovation adaptive EKF for in-flight alignment of airborne POS," *IEEE Trans. Instrum. Meas.*, vol. 60, no. 4, pp. 1378–1388, Apr. 2011.
- [32] Y. Huang, Y. Zhang, Y. Zhao, and J. Chambers, "A novel robust Gaussian-student's t mixture distribution based Kalman filter," *IEEE Trans. Signal Process.*, vol. 67, no. 13, pp. 3606–3620, Jul. 2019.
- [33] C. Hide, T. Moore, and M. Smith, "Adaptive Kalman filtering algorithms for integrating GPS and low cost INS," in *Proc. Position Location Navigat. Symp. (PLANS)*, Apr. 2004, pp. 227–233.
- [34] M.-J. Yu, "INS/GPS integration system using adaptive filter for estimating measurement noise variance," *IEEE Trans. Aerosp. Electron. Syst.*, vol. 48, no. 2, pp. 1786–1792, Apr. 2012.
- [35] S. Sarkka and A. Nummenmaa, "Recursive noise adaptive Kalman filtering by variational Bayesian approximations," *IEEE Trans. Autom. Control*, vol. 54, no. 3, pp. 596–600, Mar. 2009.
- [36] G. Agamennoni, J. I. Nieto, and E. M. Nebot, "Approximate inference in state-space models with heavy-tailed noise," *IEEE Trans. Signal Process.*, vol. 60, no. 10, pp. 5024–5037, Oct. 2012.
- [37] S. Särkkä Jouni Hartikainen, "Variational Bayesian adaptation of noise covariances in non-linear Kalman filtering," 2013, *arXiv:1302.0681*. [Online]. Available: <http://arxiv.org/abs/1302.0681>
- [38] Y. Huang, Y. Zhang, Z. Wu, N. Li, and J. Chambers, "A novel adaptive Kalman filter with inaccurate process and measurement noise covariance matrices," *IEEE Trans. Autom. Control*, vol. 63, no. 2, pp. 594–601, Feb. 2018.
- [39] Y. Huang, Y. Zhang, B. Xu, Z. Wu, and J. A. Chambers, "A new adaptive extended Kalman filter for cooperative localization," *IEEE Trans. Aerosp. Electron. Syst.*, vol. 54, no. 1, pp. 353–368, Feb. 2018.
- [40] C. M. Bishop, *Pattern Recognition and Machine Learning (Information Science and Statistics)*. New York, NY, USA: Springer-Verlag, 2006.
- [41] Z. Yang and Z. Ge, "Industrial virtual sensing for big process data based on parallelized nonlinear variational Bayesian factor regression," *IEEE Trans. Instrum. Meas.*, vol. 69, no. 10, pp. 8128–8136, Oct. 2020.
- [42] K. Y. Leung, Y. Halpern, T. D. Barfoot, and H. H. Liu, "The UTIAS multi-robot cooperative localization and mapping dataset," *Int. J. Robot. Res.*, vol. 30, no. 8, pp. 969–974, Jul. 2011.



Yulong Huang (Member, IEEE) received the B.S. degree in automation and the Ph.D. degree in control science and engineering from the College of Automation, Harbin Engineering University (HEU), Harbin, China, in 2012 and 2018, respectively.

From November 2016 to November 2017, he was a Visiting Graduate Researcher at the Electrical Engineering Department, Columbia University, New York, NY, USA. Currently, he is an Associate Professor of navigation, guidance, and control with HEU. From December 2019 to December 2021, he will be associated with the Department of Mechanical Engineering, The City University of Hong Kong, Hong Kong, as a Hong Kong Scholar. His current research interests include signal processing, information fusion, and their applications in navigation technology, such as inertial navigation and integrated navigation.

Dr. Huang was a recipient of excellent doctoral thesis from the Chinese Association of Automation (CAA) in 2019.



Chao Xue is currently pursuing the master's degree with the College of Intelligent Systems Science and Engineering, Harbin Engineering University, Harbin, China.

His current research interests include signal processing, information fusion, and their applications in navigation technology, such as cooperative navigation, inertial navigation, and integrated navigation.



Fengchi Zhu is currently pursuing the master's degree with the College of Intelligent Systems Science and Engineering, Harbin Engineering University, Harbin, China.

His current research interests include signal processing, information fusion, and their applications in navigation technology, such as cooperative navigation, inertial navigation, and integrated navigation.



Wenwu Wang (Senior Member, IEEE) received the B.Sc., M.E., and Ph.D. degrees from the College of Automation, Harbin Engineering University, Harbin, China, in 1997, 2000, and 2002, respectively.

He then worked in King's College London, London, U.K., from 2002 to 2003, Cardiff University, Cardiff, U.K., from 2004 to 2005, Tao Group Ltd. (now Antix Labs Ltd.) from 2005 to 2006, Creative Labs from 2006 to 2007, before joining the University of Surrey, Surrey, U.K., in May 2007, where he is a Professor in signal processing and

machine learning and the Co-Director of the Machine Audition Lab, Centre for Vision Speech and Signal Processing. He is also a Guest Professor at the Qingdao University of Science and Technology, Qingdao, China. He was a Visiting Scholar at The Ohio State University, Columbus, OH, USA, in 2008. His current research interests include blind signal processing, sparse signal processing, audiovisual signal processing, machine learning and perception, artificial intelligence, machine audition (listening), and statistical anomaly detection. He has (co)-authored over 250 publications in these areas.

Dr. Wang was a (co)-recipient of the Judge's Award on DCASE 2020, the Reproducible System Award on DCASE 2019 and DCASE 2020, the Best Student Paper Award on LVA/ICA 2018, the Best Oral Presentation on FSDM 2016, the Top 10% Paper Award in the IEEE ICME 2015, the Best Student Paper Award finalists on ICASSP 2019 and LVA/ICA 2010, the TVB Europe Award for Best Achievement in Sound in 2016, and the Best Solution Award on the Dstl Challenge "Under-sampled Signal Recognition" in 2012, and achieved the First Place in the 2020 DCASE challenge on "Urban Sound Tagging with Spatio-Temporal Context," and the First Place in the 2017 DCASE Challenge on "Large-scale Weakly Supervised Sound Event Detection for Smart Cars." He was the Publication Co-Chair for ICASSP 2019, Brighton, U.K. Since 2021, he has been elected as a member of the IEEE Signal Processing Theory and Methods Technical Committee and the IEEE Machine Learning for Signal Processing Technical Committee. Since 2019, he also serves as a member of the International Steering Committee of Latent Variable Analysis and Signal Separation. He has been a Senior Area Editor since 2019 and an Associate Editor from 2014 to 2018 of the IEEE TRANSACTIONS ON SIGNAL PROCESSING. Since 2020, he has been an Associate Editor of the IEEE/ACM TRANSACTIONS ON AUDIO SPEECH AND LANGUAGE PROCESSING, and an Associate Editor of the *EURASIP Journal on Audio Speech and Music Processing* since 2019. He has been a Specialty Editor-in-Chief of *Frontiers in Signal Processing* since 2020.



Yonggang Zhang (Senior Member, IEEE) received the B.S. and M.S. degrees from the College of Automation, Harbin Engineering University (HEU), Harbin, China, in 2002 and 2004, respectively, and the Ph.D. degree in electronic engineering from Cardiff University, Cardiff, U.K., in 2007.

He worked as a Post-Doctoral Fellow at Loughborough University, Loughborough, U.K., from 2007 to 2008, in the area of adaptive signal processing. Currently, he is a Professor of navigation, guidance, and control with HEU. His current research interests

include signal processing, information fusion, and their applications in navigation technology, such as fiber optical gyroscope, inertial navigation, and integrated navigation.



Jonathon A. Chambers (Fellow, IEEE) received the Ph.D. and D.Sc. degrees in signal processing from the Imperial College of Science, Technology and Medicine, Imperial College London, London, U.K., in 1990 and 2014, respectively.

From 1991 to 1994, he was a Research Scientist with the Schlumberger Cambridge Research Center, Cambridge, U.K. In 1994, he returned to Imperial College London as a Lecturer in signal processing and was promoted to Reader (Associate Professor) in 1998. From 2001 to 2004, he was the Director of

the Center for Digital Signal Processing and a Professor of signal processing with the Division of Engineering, King's College London, London. From 2004 to 2007, he was a Cardiff Professorial Research Fellow with the School of Engineering, Cardiff University, Cardiff, U.K. From 2007 to 2014, he led the Advanced Signal Processing Group, School of Electronic, Electrical and Systems Engineering, Loughborough University, Loughborough, U.K., and is now a Visiting Professor. In 2015, he joined the School of Electrical and Electronic Engineering, Newcastle University, Newcastle upon Tyne, U.K., where he was a Professor of signal and information processing and led the ComS2IP Group and is now a Visiting Professor. In 2017, he became the Head of the Department of Engineering, University of Leicester, Leicester, U.K. He is also an International Honorary Dean and a Guest Professor at Harbin Engineering University, Harbin, China, with support from the 1000 Talents Scheme. He has coauthored the books *Recurrent Neural Networks for Prediction: Learning Algorithms, Architectures and Stability* (New York, NY, USA: Wiley, 2001) and *EEG Signal Processing* (New York, NY, USA: Wiley, 2007). He has advised approaching 100 researchers through to Ph.D. graduation and published more than 600 conference papers and journal articles, many of which are in IEEE journals. His research interests include adaptive and blind signal processing and their applications.

Dr. Chambers is a fellow of the Royal Academy of Engineering, U.K., and the Institution of Electrical Engineers. He has served on the IEEE Signal Processing Theory and Methods Technical Committee for six years and the IEEE Signal Processing Society Awards Board for three years. He also served as a member of the IEEE Signal Processing Conference Board and the European Signal Processing Society Best Paper Awards Selection Panel. He was the Technical Program Chair of the 15th International Conference on Digital Signal Processing and the 2009 IEEE Workshop on Statistical Signal Processing, both held in Cardiff, U.K., and a Technical Program Co-Chair for the 36th IEEE International Conference on Acoustics, Speech, and Signal Processing, Prague, Czech Republic. He received the first QinetiQ Visiting Fellowship in 2007 for his outstanding contributions to adaptive signal processing and his contributions to QinetiQ, as a result of his successful industrial collaboration with the international defense systems company QinetiQ. He additionally served as an Associate Editor for the IEEE TRANSACTIONS ON SIGNAL PROCESSING for three terms over the periods 1997–1999 and 2004–2007 and as a Senior Area Editor from 2011 to 2014.